NOAA Technical Report NOS 89

The Response of the Shelf to Hurricane Belle August 1976

Rockville,Md.
August 1981

U.S. DEPARTMENT OF COMMERCE
National Oceanic and Atmospheric Administration
National Ocean Survey

NOAA TECHNICAL REPORTS

National Ocean Survey Series

rvey (NOS) provides charts and related information for the safe navigation of
e. The survey also furnishes other Earth science data--from geodetic, hydro-
, gravimetric, and astronomic surveys, observations, investigations, and mea-
ife and property and to meet the needs of engineering, scientific, defense,
al interests.

reports deal with new practices and techniques, the views expressed are those of
necessarily represent final survey policy. NOS series NOAA Technical Reports is
retains the consecutive numbering sequence of, the former series, Environmental
istration (ESSA) Technical Reports Coast and Geodetic Survey (C&GS), and the ear-
lier series, C&GS Technical Bulletins.

Microfiche for the following reports is available from the National Technical Information Service (NTIS), U.S. Department of Commerce, Sills Bldg., 5285 Port Royal Road, Springfield, VA 22161. (NTIS accession numbers given in parentheses.) Write to source for price.

NOAA TECHNICAL REPORTS

NOS 50 Pacific SEAMAP 1961-70 Data for Areas 16524-10 and 17524-10: Longitude 165°W to 180°, Latitude 24°N to 30°N, bathymetry, magnetics, and gravity. E. F. Chiburis, J. J. Dowling, P. Dehlinger, and M. J. Yellin, July 1972. (COM-73-50172)

NOS 51 Pacific SEAMAP 1961-70 Data for Areas 15636-12, 15642-12, 16836-12, and 16842-12: Longitude 156°W to 180°, Latitude 36°N to 48°N, bathymetry, magnetics, and gravity. E. F. Chiburis, J. J. Dowling, P. Dehlinger, and M. J. Yellin, July 1972. (COM-73-50280)

NOS 52 Pacific SEAMAP 1961-70 data evaluation summary. P. Dehlinger, E. F. Chiburis, and J. J. Dowling, July 1972. (COM-73-50110)

NOS 53 Grid calibration by coordinate transfer. Lawrence Fritz, December 1972. (COM-73-50240)

NOS 54 A cross-coupling computer for the Oceanographer's Askania Gravity Meter. Carl A. Pearson and Thomas E. Brown, February 1973. (COM-73-50317)

NOS 55 A mathematical model for the simulation of a photogrammetric camera using stellar control. Chester C. Slama, December 1972. (COM-73-50171)

NOS 56 Cholesky factorization and matrix inversion. Erwin Schmid, March 1973. (COM-73-50486)

NOS 57 Complete comparator calibration. Lawrence W. Fritz, July 1973. (COM-74-50229)

NOS 58 Telemetering hydrographic tide gauge. Charles W. Iseley, July 1973. (COM-74-50001)

NOS 59 Gravity gradients at satellite altitudes. B. Chovitz, J. Lucas, and F. Morrison, November 1973. (COM-74-50231)

NOS 60 The reduction of photographic plate measurements for satellite triangulation. Anna-Mary Bush, June 1973. (COM-73-50749)

NOS 61 Radiation pressure on a spheroidal satellite. James R. Lucas, July 1974. (COM-74-51195/AS)

NOS 62 Earth's gravity field and station coordinates from Doppler Data, Satellite Triangulation, and Gravity Anomalies. Karl-Rudolf Koch, February 1974. (COM-74-50490/AS)

NOS 63 World maps on the August epicycloidal conformal projection. Erwin Schmid, May 1974. (COM-74-11746/AS)

NOS 64 Variability of tidal datums and accuracy in determining datums from short series of observations. Robert Lawrence Swanson, October 1974. (COM-75-10275)

NOS 65 NGS-1. The statistics of residuals and the detection of outliers. Allen J. Pope, May 1976, 133 pp. (PB258428)

NOS 66 NGS-2. Effect of geoceiver observations upon the classical triangulation network. Robert E. Moose, and Soren W. Henriksen, June 1976, 65 pp. (PB260921)

(Continued on inside back cover)

NOAA Technical Report NOS 89

The Response of the Shelf to Hurricane Belle

August 1976

Richard C. Patchen
Bernard W. Gottholm

Office of Oceanography
National Ocean Survey
Rockville, Md.
August 1981

U.S. DEPARTMENT OF COMMERCE
Macolm Baldrige, Secretary

National Oceanic and Atmospheric Administration
John V. Byrne, Administrator

National Ocean Survey
Rear Admiral Herbert R. Lippold, Jr., Director

Mention of a commercial company or product does not constitute an endorsement by NOAA/National Ocean Survey. Use for publicity or advertising purposes of information from this publication concerning proprietary products is not authorized.

Contents

List of Tables

THE RESPONSE OF THE SHELF TO HURRICANE BELLE AUGUST 1976

Richard C. Patchen and Bernard W. Gottholm*

ASTRACT.—On 10 August 1976 Hurricane Belle passed through the New York Bight; the data set included meteorological information from the National Weather Service, water level information from the National Ocean Survey, and current meter and Salinity/Temperature/Depth (STD) information from the Marine Ecosystem Analysis Program. Hurricane Belle can be classified as a fast-moving storm translating over a two-layer density structure. The temporal and spatial responses to the hurricane were determined by spectral and residual techniques. The STD information and the temperature records obtained at the current meter locations indicate that a cooling and mixing of the surface waters was observed at stations to the right of the storm, and that only weak mixing was observed at stations directly in the path of the storm. At current meter locations on deeper areas of the continental shelf (greater than 55 m), the baroclinic response of a generation of internal inertia-gravity waves in the lee of the hurricane can be seen in the two layers. For stations on the shallower area of the shelf (less than 55 m), a strong barotropic response indicated by the generation of localized quasi-geostrophic barotropic Rossby waves, 18 to 20 hours after the hurricane entered the New York Bight, is observed. The data compared favorably with the results of Chang and Anthes for a hurricane translating at 11 m s^{-1}. The topographic restraint on the velocity field for stations located in the Hudson Canyon is described.

INTRODUCTION

Understanding the response of the continental shelf to the passage of a hurricane is important, because this understanding leads to the realization of the possibility of prediction. The loss of life and money resulting from the passage of a hurricane or other severe meteorological event is well documented. Hurricane Agnes in 1972 caused $20 million in property damage in the Tampa-St. Petersburg area alone. Therefore, the prediction of the path alone would have been of significant benefit. The description of the response of the continental shelf is complicated by the various spatial and temporal modes within one given region. The response of the impulse to the meteorological event is dependent on (1) the pre-event density regime, (2) the bathymetric variability for a given region, and (3) the classification of the impulse itself, including the wind profile and translation speed. Theoretical investigations have attempted to (1) fully describe the various atmospheric impulses and (2) explain descriptively, analytically, and numerically the oceanographic response, including the intensive mixing and upwelling which accompanies the passage of a storm.

Numerous articles have been written describing the barotropic and baroclinic response on the water column resulting from the passage of a hurricane. Initial theoretical work by O'Brien and Reid (1967), and O'Brien (1967), emphasized first the linear, then the nonlinear response to a stationary axially symmetric hurricane. Research was further conducted both by O'Brien (1968) and Geisler (1970) on the dynamic response to a translating hurricane. Recent analytical and numerical papers emphasizing the baroclinic as well as barotropic response to translating hurricanes other than those that are axially symmetric include: Geisler and Dickerson (1972), Kraus (1972), Elsberry et al. (1976), Ichiye (1977), and Chang and Anthes (1978).

For any theoretical models, either analytical or numerical, the results must be verified by the data collected. However, the data collected during the passage of a strong hurricane are extremely limited and difficult to obtain. The data collected is mainly limited to quasi-stationary, slow-moving hurricanes: Hilda in 1964, reported by Leipper (1967), Betsy in 1965, reported by Landis and Leipper (1968), and Ginger in

*Employed by the Office of Oceanography within the National Ocean Survey, National Oceanic and Atmospheric Administration, U.S. Department of Commerce.

1971, reported by Black and Mallinger (1972). However, during Hurricane Belle in 1976, the New York Bight was highly instrumented from various sources. Data are available from the National Weather Services (NWS) within the National Oceanic and Atmospheric Administration (NOAA), NOAA's Environmental Research Laboratories (ERL), NOAA's Marine Ecosystems Analysis (MESA) New York Bight Project, and NOAA's National Ocean Survey (NOS) extensive tide program. Using the data collected from those sources of instrumentation, the opportunity existed to perform a complete synthesis of the various physical parameters measured in the New York Bight.

DESCRIPTION OF THE DATA BASE

On 6 August 1976, Hurricane Belle formed about 250 nautical miles east-northeast of Nassau. The system intensified to a central pressure of 957 mbs with a sustained wind speed of 105 knots. It moved northeast, parallel to the coast, and finally hit land on 10 August at 0500 hours GMT on the southern coast of Long Island, N.Y. Figures 1 and 2 indicate the locations of the various parameters measured in the region, and the path of Hurricane Belle is plotted on the charts. NOAA's Environmental Buoy EB-41 (at 38.7°N, 73.6°W), and the NWS weather station at Kennedy Airport are indicated on figure 1. Unfortunately, the data set at EB-34 (at 40.1°N, 73.3°W) is questionable because the buoy, which was located directly in the path of Hurricane Belle, broke loose. The seven current meter moorings and the STD casts were part of the MESA New York Bight Project observational program. The current meters on the seven moorings were also equipped with temperature sensors. The water level information was collected as part of the NOS tide observational program.

Table 1 indicates the station locations for the MESA current meter locations, including geographic position, depth of the station, observational depths, number of days of recoverable data, and sensors in operation. The observational level indicated by SPAR is a current meter suspended from a surface buoy, approximately 3 m below the surface. Other observational depths are referenced to the bottom. Data were collected using a subsurface mooring configuration with Aanderaa current meters attached at discrete depths to a wire rope with an acoustic or explosive bolt release between the bottom meter and the anchor.

Meteorological data were compiled from various sources within NWS. The data from EB-41 were obtained from Sallie P. Ward, of Sperry Support Services, Bay St. Louis, Miss. Sperry Support Services was responsible for the initial processing of the Environmental Buoy tapes. The path of Hurricane Belle was reported in *Hurricane Belle, Climatological Data National Summary,* and the information at John F. Kennedy Airport (JFK) was digitized from the *Local Climatological Data, Monthly Summary* for June-October 1976.

Deep sea tide data were collected as part of NOAA's Delaware/Maryland/Virginia/North Carolina (DELMARVANC) Hydrographic Survey (June-November 1976) and NOS Offshore Telemetering Tide System (OTTS). Results from the OTTS I and OTTS II gages were reported by Gill and Porter (1978). Tide information is also available for both Atlantic City and Sandy Hook, N.J. Unfortunately, tide information is not available along the southern coast of Long Island, N.Y.

The STD data were collected as part of the MESA New York Bight Project's Extended Water Characterization Cruises (XWCC) and were reported by Starr et al. (1977), and Hazelworth et al. (1977). The data preceding the hurricane were obtained during the XWCC 10 cruise on 30 June-1 July 1976; and the data after the hurricane passed through the New York Bight were obtained during the XWCC 11 on 12-16 September 1976.

DATA ANALYSIS

The Office of Oceanography's Circulatory Surveys Branch within NOS was responsible for the processing of the current meter information. After deployment and recovery of the data tapes from the current meter program, the tapes were transcribed or translated to a computer-compatible format. Times were assigned to all usable data files, and after all erroneous records from instrument malfunctions were removed, the data tapes were sent to the National Oceanographic Data Center (NODC) of the Environmental Data and Information Service (EDIS) for archival storage and to NOAA's Atlantic Oceanographic and Meteorological Laboratory (AOML).

To isolate the response of the circulation to the passage of Hurricane Belle, a record was required with the tidal signal removed (without filtering the response to the hurricane). A residual time series record defined as the original series minus the predicted series was derived. Also, the residual series which best represents the response to the storm was determined to be the component series resolved both along and at a 90-degree angle to Belle's path. The predicted series was determined by performing a 15-day harmonic analysis up to the time Belle entered the New York Bight. This ensures the analysis will not be biased by the hurricane. Spectral analyses were also performed on all original series, using the method described by Cooley and Tukey (1965).

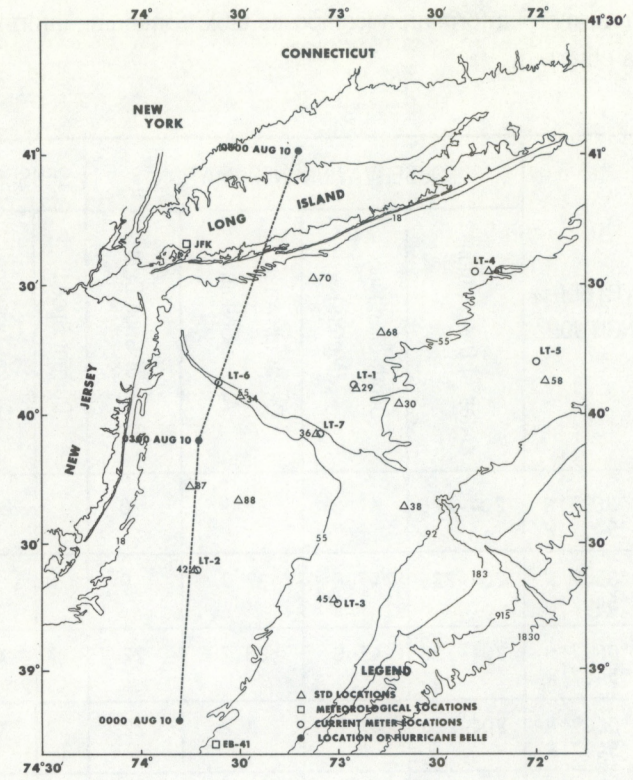

Figure 1. —A chart indicating the locations of current meter, STD, and meteorological observations collected during the passage of Hurricane Belle. The path of the hurricane is also indicated on the chart.

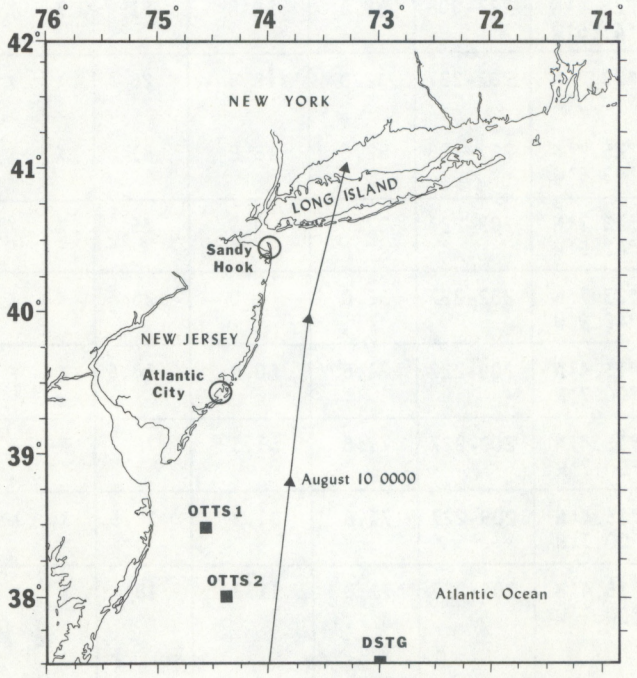

Figure 2. —A chart indicating the location of the water level observations collected during the passage of Hurricane Belle. The path of the hurricane is also indicated on the chart.

Table 1.—Current meter information (composite table containing information relating to data observed).

STATION NO.	LATITUDE LONGITUDE	OBSERVATION INFORMATION				SENSORS IN OPERATION				
		Dates of Observations	Depth of Station (Meters)	Depth of Meter Above Bottom	Days of Good Data	Current Speed	Current Direction	Temperature	Conductivity	Pressure
LT-1S	40°06.7'N 72°54.7'W	204-226	47.8	SPAR	0					
LT-1A	40°06.7'N 72°54.7'W	204-226	47.8	37.7	0					
LT-1B	40°06.7'N 72°54.7'W	204-226	47.8	28.2	22	X	X	X		X
LT-1C	40°06.7'N 72°54.7'N	204-226	47.8	8.2	22	X	X	X		X
LT-1D	40°06.7'N 72°54.7'W	204-226	47.8	1.0	22	X	X	X		X
LT-2S	39°25.4'N 73°42.6'W	202-227	32.0	SPAR	0					
	39°25.4'N 73°43.5'W	227-308	32.6	SPAR	81	X	X	X	X	X
LT-2A	39°23.7'N 73°42.9'W	202-227	32.0	18.8	25	X	X	X	X	X
	39°25.2'N 73°43.5'W	227-308	32.6	18.8	81	X	X	X	X	X
LT-2B	39°23.7'N 73°42.9'W	202-227	32.0	9.3	25	X	X	X	X	X
LT-2C	39°23.7'N 73°42.9'W	202-227	32.0	1.0	25	X	X	X	X	X
LT-3A	39°15.4'N 73°00.7'W	209-227	71.6	60.9	18.5	X	X	X		X
LT-3B	39°15.4'N 73°00.7'W	209-227	71.6	51.3	18	X	X	X		X
LT-3C	39°15.4'N 73°00.7'W	209-227	71.6	31.3	18.5	X	X	X	X	X
LT-3D	39°15.4'N 73°00.7'W	209-227	71.6	11.3	18	X	X	X		X

Table 1.—Current meter information (composite table containing information relating to data observed). - Continued

STATION NO.	LATITUDE LONGITUDE	OBSERVATION INFORMATION				SENSORS IN OPERATION				
		Dates of Observations	Depth of Station (Meters)	Depth of Meter Above Bottom	Days of Good Data	Current Speed	Current Direction	Temperature	Conductivity	Pressure
LT-4S	40°33.4'N 72°18.3'W	203-226	50.8	SPAR	23	X	X	X		X
LT-4A	40°33 4'N 72°18.3'W	203-226	50.8	27.6	23	X	X	X	X	X
	40°33.4'N 72°18.3'W	226-302	50.8	27.6	76	X	X	X	X	X
LT-4B	40°33.4'N 72°18.3'W	203-226	50.8	7.6	22.5	X	X	X	X	X
	40°33.4'N 72°18.3'W	226-302	50.8	7.6	0					
LT-4C	40°33.4'N 72°18.3'	203-226	50.8	1.0	23	X	X	X		X
	40°33.4'N 72°18.3'W	226-302	50.8	1.0	76	X	X	X		X
LT-5A	40°11.9'N 72°01.0'W	203-226	64.6	45.9	23.3	X	X	X	X	X
LT-5B	40°11.9'N 72°01.0'W	203-226	64.6	25.9	23.3	X	X	X	X	X
LT-5C	40°11.9'N 72°01.0'W	203-226	64.6	5.9	23.2	X	X	X		X
LT-5D	40°11.9'N 72°01.0'W	203-226	64.6	1.0	0					
LT-6S	40°07.6'N 73°37.6'W	202-225	71.6	SPAR	24	X	X	X	X	X
LT-6A	40°07.5'N 73°37.8'W	202-225	71.6	48.3	24	X	X	X		X
LT-6B	40°07.5'N 73°37.5'W	202-225	71.6	28.3	24	X	X	X	X	X
LT-6C	40°07.5'N 73°36.8'W	202-225	71.6	18.3	0					

Table 1.—Current meter information (composite table containing information relating to data observed).— Continued

STATION NO.	LATITUDE LONGITUDE	OBSERVATION INFORMATION				SENSORS IN OPERATION				
		Dates of Observations	Depth of Station (Meters)	Depth of Meter Above Bottom	Days of Good Data	Current Speed	Current Direction	Temperature	Conductivity	Pressure
LT-6D	40° 07.5'N 73° 36.8'W	202-225	71.6	8.3	0					
LT-6E	40° 07.5'N 73° 36.8'W	202-225	71.6	1.0	0					
LT-7S	39°55.5'N 73°05.2'W	202-225	66.2	SPAR	24	X	X	X	X	X
LT-7A	39°55.5'N 73°05.2'W	202-225	66.2	48.3	24	X	X	X	X	X
	39°55.5'N 73°05.3'W	226-301	66.2	48.3	76	X	X	X	X	X
LT-7B	39°55.5'N 73°05.2'W	202-225	66.2	28.2	24	X	X	X	X	X
	39°55.5'N 73°05.3'W	226-301	66.2	28.2	76	X	X	X		X
LT-7C	39°55.5'N 73°05.2'W	202-225	55.2	18.3	24	X	X	X		X
	39°55.5'N 73°05.3'W	226-301	66.2	18.3	76	X	X	X	X	X
LT-7D	39°55.5'N 73°05.2'W	202-225	66.2	8.3	24	X	X	X	X	X
	39°55.5'N 73°05.3'W	226-301	66.2	8.3	76	X	X	X	X	X
LT-7E	39°55.5'N 73°05.2'W	202-222	66.2	1.0	21	X	X	X		X
	39°55.5'N 73°05.3'W	226-301	66.2	1.0	76	X	X	X		X

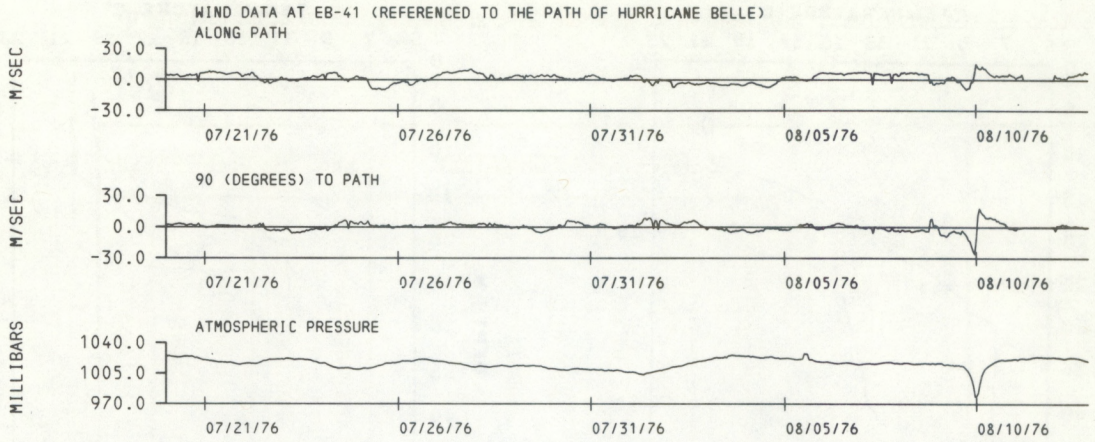

Figure 3. —A plot of the wind and pressure observation at EB-41 where the positive component along the path is 5 degrees (True) and a positive component at a 90-degree angle to the path is 95 degrees (True).

The raw meteorological data at hourly intervals for EB-41 were obtained from Sperry Rand Corporation, and the information at 3-hour intervals for the meteorological stations at JFK Airport was digitized from NWS summaries. For both records, the wind velocities were resolved both along and at a 90-degree angle to the path of the hurricane. The results from EB-41 and JFK were almost identical, with slightly higher velocities at JFK. Figure 3 represents the wind and pressure response at EB-41 to the passage of the hurricane. A positive component along the path is 5 degrees (true) and a positive component at a 90-degree angle to the path is 95 degrees (true).

Processed tide data were obtained from NOS for the Deep Sea Tide Gage (DSTG), OTTS gages, and the land-based tide stations. Residual series of the tide records for Atlantic City and Sandy Hook, N.J., were also determined. The STD data were obtained directly from the XWCC reports, and residual records for the observed temperature data from the Aanderaa current meters were calculated.

WATER COLUMN RESPONSE

Leipper (1967), Hazelworth (1968), and other reports on the response of the water column to the passage of a hurricane were mainly limited to sea surface temperatures, bathythermographs (BT), and a few hydrographic casts. Their results are applicable mainly to slow-moving storms. Observations indicate upwelling along the path of the storm, advection of the surface layer, cooling and mixing of the surface layer, and convergence and downwelling around the hurricane area. The data collected during the passage of Hurricane Belle are shown in figure 4. Temperature versus depth information at the seven current meter locations is plotted. The solid trace is the information from XWCC 10 at the closest available STD cast (or casts for stations LT2, LT4, and LT5), and the dashed trace is from XWCC 11. The current meter stations and observational depth are indicated on the right axis for each plot. The squares are the residual temperatures directly before, and the triangles are the residual temperatures after the passage of Hurricane Belle. The response of the hurricane is seen vertically from surface to the bottom, at all meters; however, mixing is more intense for observations in and above the thermocline. At stations LT3, LT4, and LT7, where near surface observations are available, a strong mixing of surface waters is indicated. At stations LT6 and LT2, directly in the path of Belle, the surface temperatures decrease only slightly, which indicates either weak mixing or possible advection along the path of the hurricane.

BAROCLINIC RESPONSE

The excitation of internal inertia-gravity waves after the passage of a severe storm has been well documented. Geisler (1970) states that the steady-state response to a storm translating at a rate greater than the baroclinic long wave speed is inertia-gravity waves in the lee of the storm. Ichiye (1977), in describing the response of a simple two-layer ocean to the passage of a slow-moving storm, neglects the generation of the inertia-gravity waves if the impulse of the storm has a time scale of longer than the inertial period. The translation speed of Belle, as it passed through the New York Bight, was approximately 11 m s^{-1}. The inertial period at 40°N latitude is approximately 18.6 hours. Table 2 represents the calculations of the baroclinic wave, Cg. The calculations for the baroclinic radius of deformation, Cg/f, were based on the STD cast from XWCC 11 that best represents the density structure at the locations of the current meters.

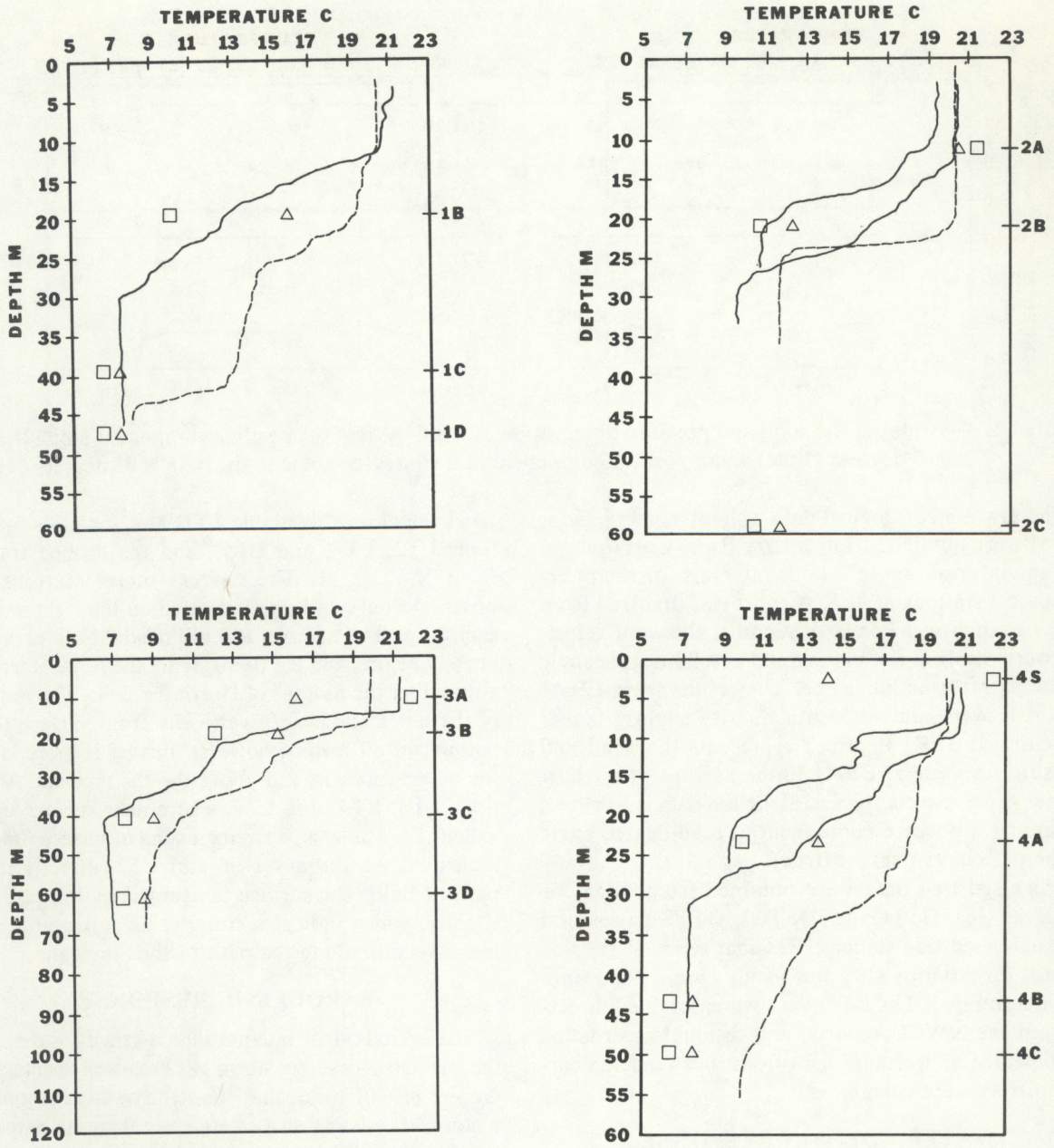

Figure 4. —Temperature vs. depth plots at the seven current meter locations. The solid trace represents information from XWCC 10. The dashed trace represents information from XWCC 11. The current meter stations at the appropriate depth are indicated on the right axis for each plot. The squares are the temperatures before, and the triangles are the temperatures after the passage of Hurricane Belle—Continued.

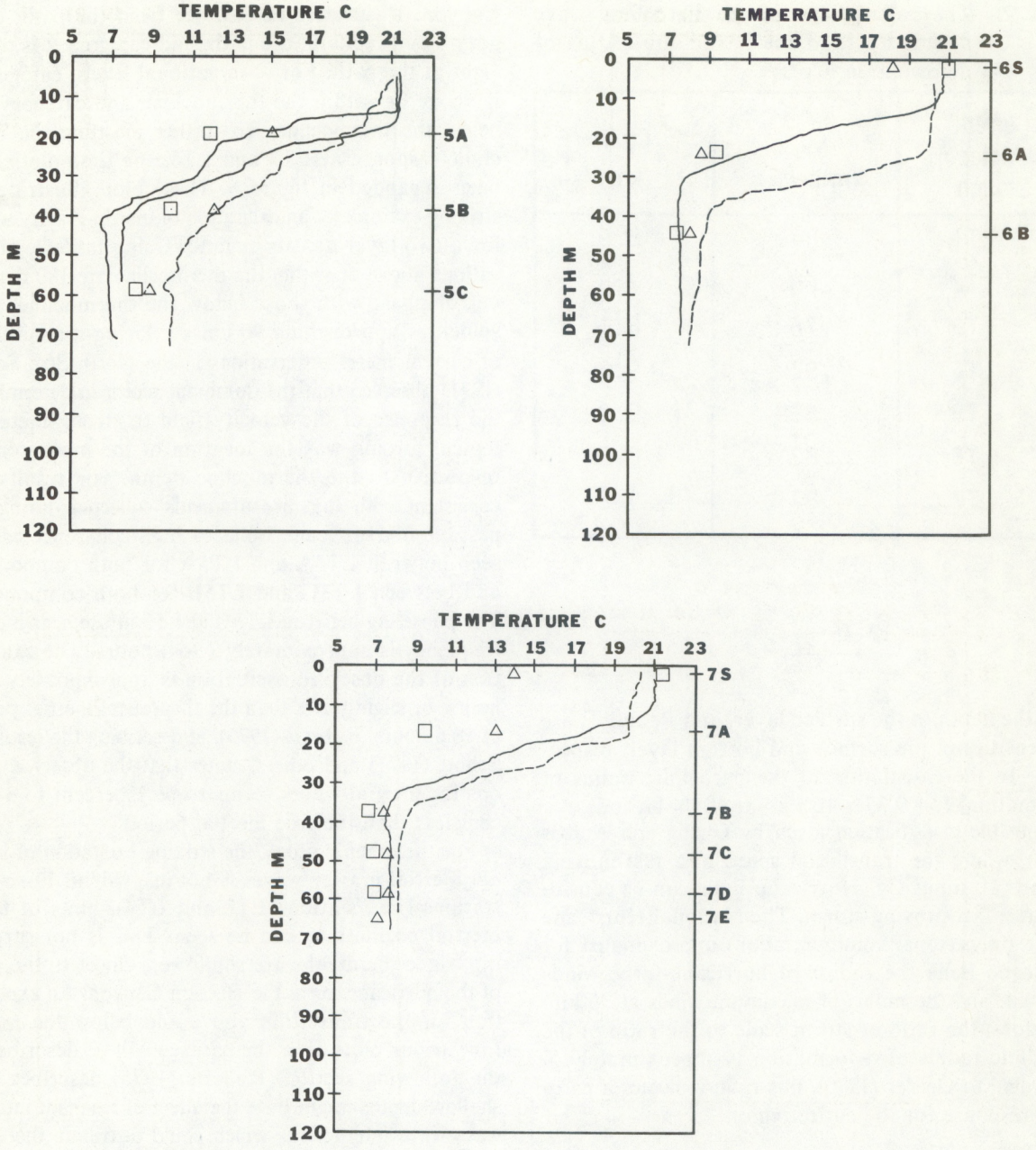

Figure 4. — Temperature vs. depth plots at the seven current meter locations.

Table 2.—The calculations of the baroclinic wave speed, Cg, and the baroclinic radius of deformation, Cg/f.

Current Meter Station	Cg (m sec^{-1})	Cg/f (km)
LT1	.84	8.9
LT2	.68	7.3
LT3	.76	8.1
LT4	.92	9.8
LT5	.85	9.0
LT6	.82	8.8
LT7	.87	9.2

$$Cg = (\varepsilon g H_1)^{1/2}$$

and

$$\varepsilon = \frac{\rho_2 - \rho_1}{\rho_2}$$

H_1 is the depth of the surface layer, and ρ_1 and ρ_2 are the densities in the surface and bottom layer, respectively. In the calculation of the baroclinic radius of deformation, f = 9.37 x 10^{-5} s^{-1} at 40°N latitude.

Using the classification given by Chang and Anthes (1978), where the translation speed of a fast-moving storm is 10 times Cg, Hurricane Belle can be considered as a fast-moving storm. The National Hurricane Center (in personal communication) approximated for Hurricane Belle the radius of hurricane-force winds at 45 km and the radius of maximum winds at 36 km. Therefore, the ratio of storm scale to the ratio of the baroclinic radius of deformation is approximately 5. According to Geisler (1970), this ratio indicates a baroclinic response for the entire region.

Time series plots

To determine the temporal response at each current meter to the passage of Hurricane Belle, the residual currents resolved both along and at a 90-degree angle to the path of the hurricane were plotted in figure 5. Using the STD cast and the temperature records on the current meters, the current meter station locations were classified by bathymetry, distance from the path of the hurricane, and observational level respective to the depth of the thermocline. Bathymetry categories are relative to the 55 m contour; category 1 is less than 55 m, and category 2 is greater than 55 m. An additional bathymetric feature for stations LT6 and LT7 is that these stations are located in the Hudson Canyon. Respective to distance from the path, category 1 is directly in the path, and category 2 is to the right of the path. For observational levels, category 1 is above or within the thermocline; and category 2 is below the thermocline. To further illustrate the baroclinic response at LT3 and LT5, the time plots have been expanded in figure 6. These plots illustrate the striking example of an excitation of inertia-gravity waves for a two-layer density regime. Using table 3, observations above or within the thermocline are 180 degrees out of phase with those below the thermocline, with velocities approaching 90 cm s^{-1}. Using a similar set of current meter observations in the North Sea, Schott (1971) observed that the dominant factor in determining the response of the velocity field to strong meteorological forcing was the location of the measurement respective to the thermocline depth. His results are consistent with the measurements collected during the passage of Hurricane Belle. A high coherence can be seen between LT3A and LT5A for both components and between LT3C and LT5B for both components. The phase lag between LT3 and LT5 at the near-inertial frequency is approximately 2 to 3 hours. The calculation of the observed oscillation is approximately 18.5 hours, or slightly less than the theoretical inertial period of 18.6 hours. Roberts (1975), in describing the results of Schott (1971) and others, states that the observed periods for inertial waves seems to be 1 percent to 3 percent less than the true inertial period.

For the other stations, the striking excitation of internal inertial-gravity waves is not as evident. For some stations (i.e., stations LT2 and LT4), hints of near-inertial oscillations can be seen. This is not surprising, since the depths are shallower, closer to the path of the hurricane, or in the Hudson Canyon. An explanation for the translation above and below the x-axes for various plots after the passage will be described in the following section. Roberts (1975) describes how shallow depths might have the effect of resonant internal wave-wave interactions which could distribute the energy to nearby frequencies.

Spectral analysis

To determine if the near-inertial waves were generated at the other station locations, spectra were calculated for each observational depth for two time periods: (1) the series up to and including the hurricane, and (2) the series up to the hurricane. A 39-hour Doodson filter was applied to the original smoothed hourly data, and spectra for the residual series for both components along and at a 90-degree angle to the path of the hurricane were calculated. Using the categories in table 3, characteristic spectra are shown in figure 7. Station LT3 again illustrates the striking example of the

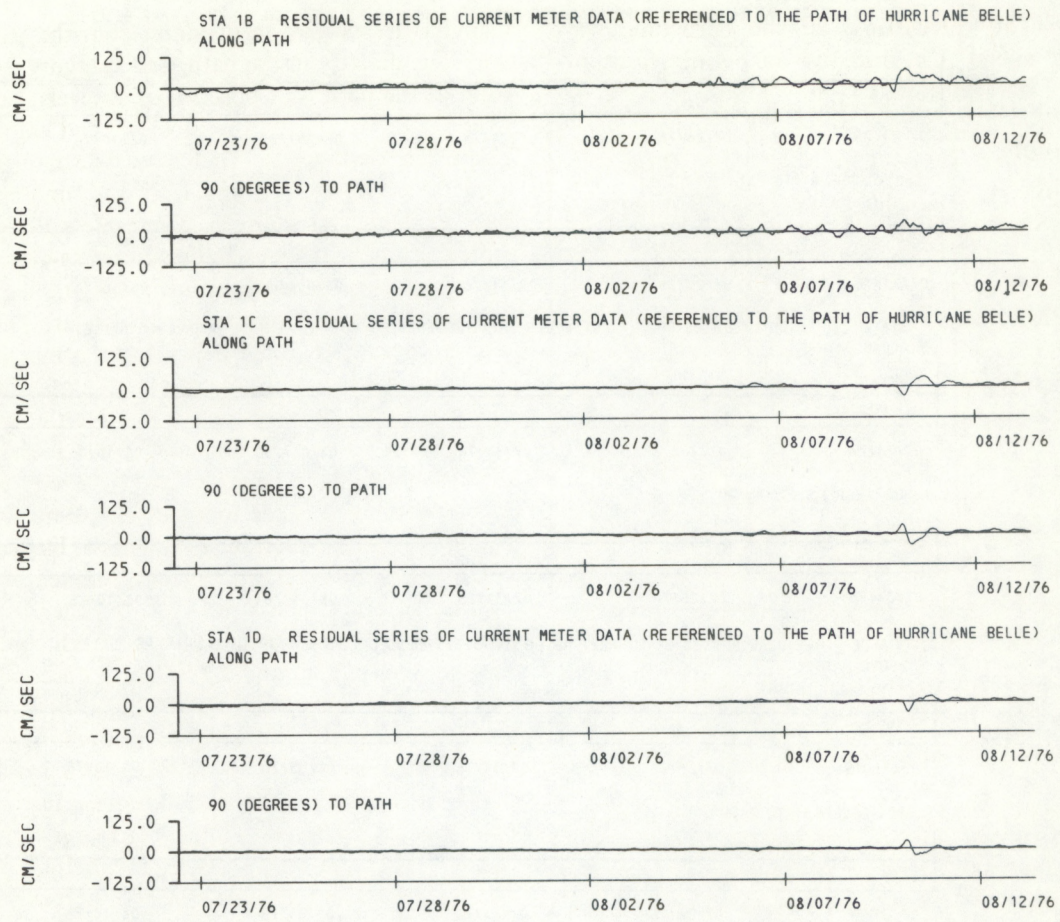

Figure 5. — Plots showing the residual currents resolved both along and at a 90-degree angle to the path of the hurricane.

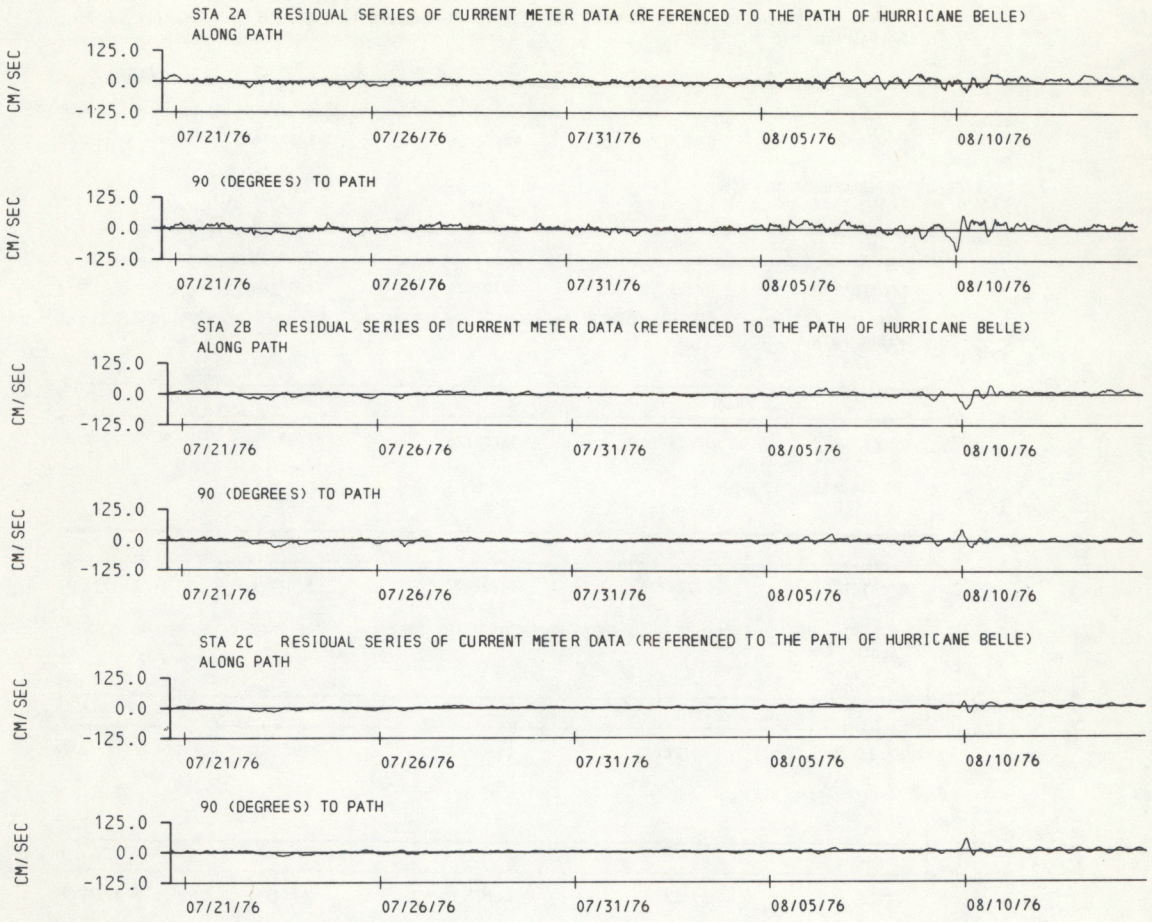

Figure 5. — Plots showing the residual currents resolved both along and at a 90-degree angle to the path of the hurricane—Continued.

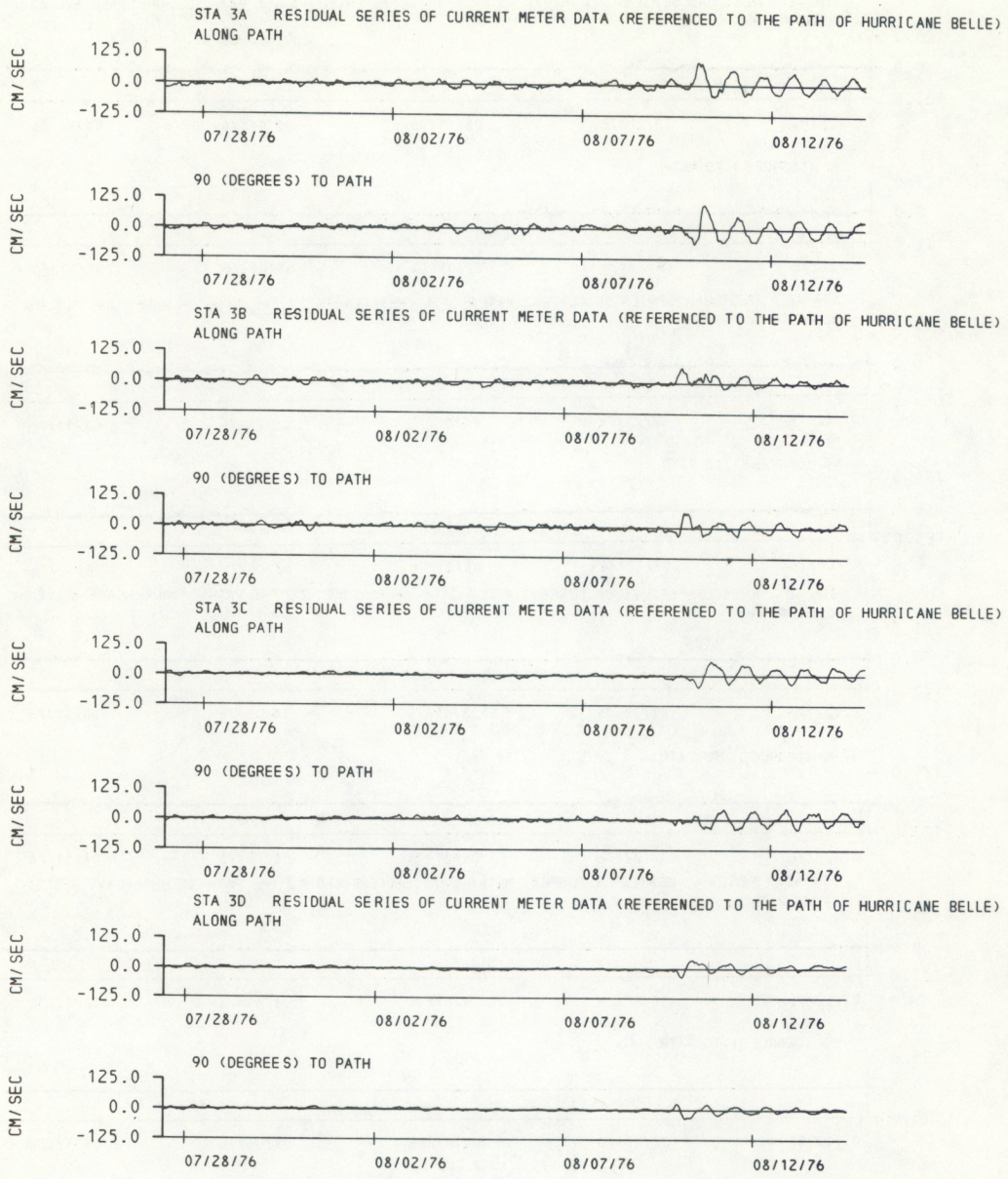

Figure 5. — Plots showing the residual currents resolved both along and at a 90-degree angle to the path of the hurricane—Continued.

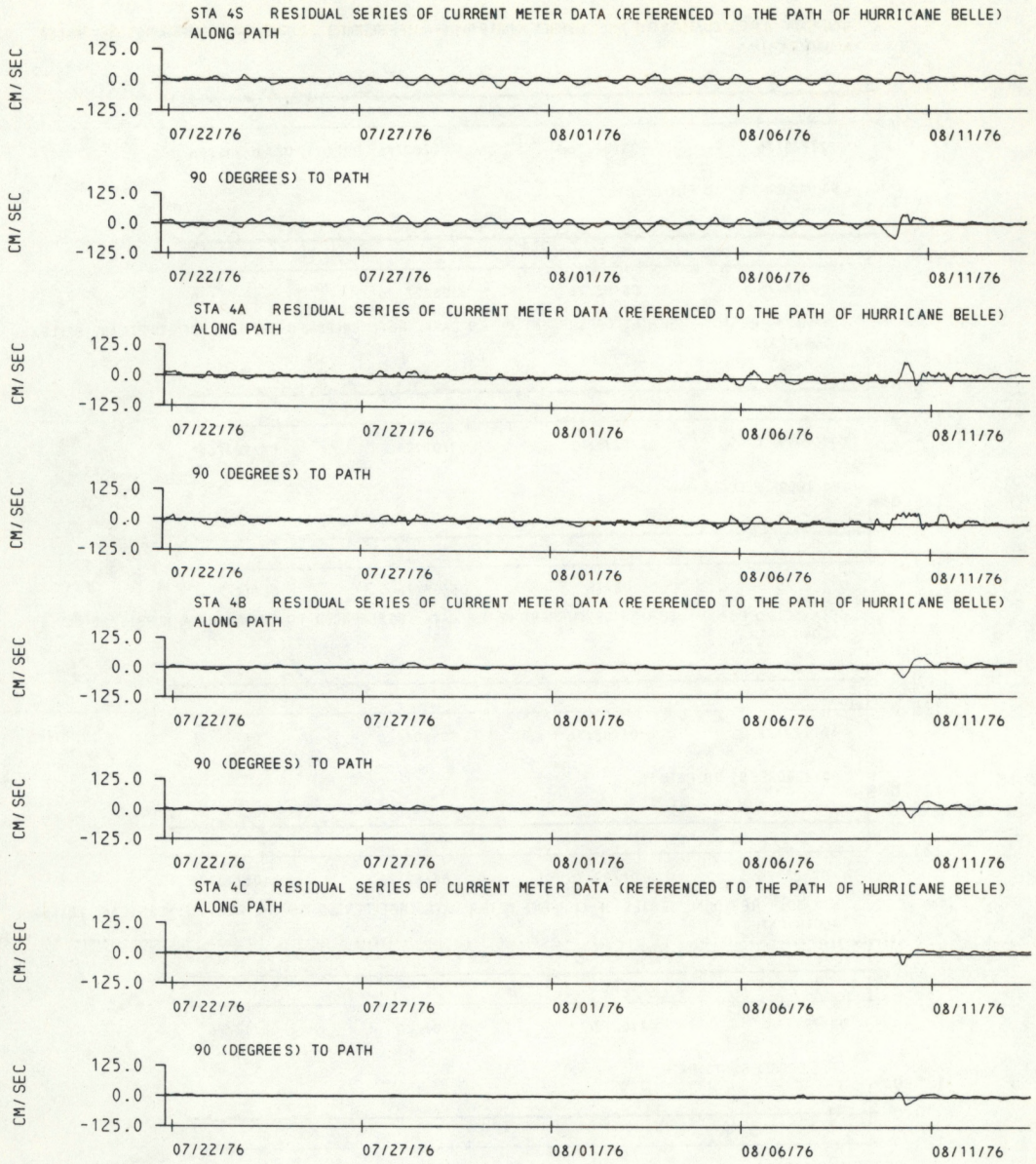

Figure 5. — Plots showing the residual currents resolved both along and at a 90-degree angle to the path of the hurricane—Continued.

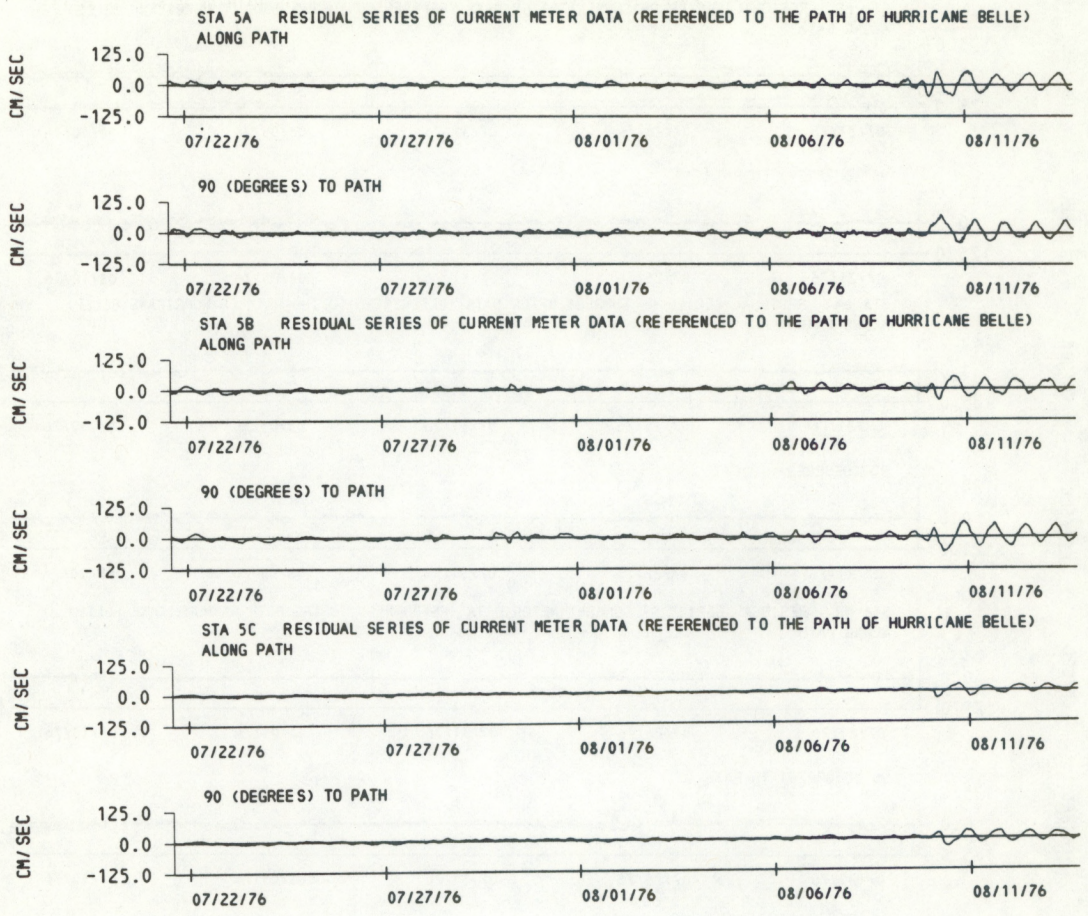

Figure 5. — Plots showing the residual currents resolved both along and at a 90-degree angle to the path of the hurricane—Continued.

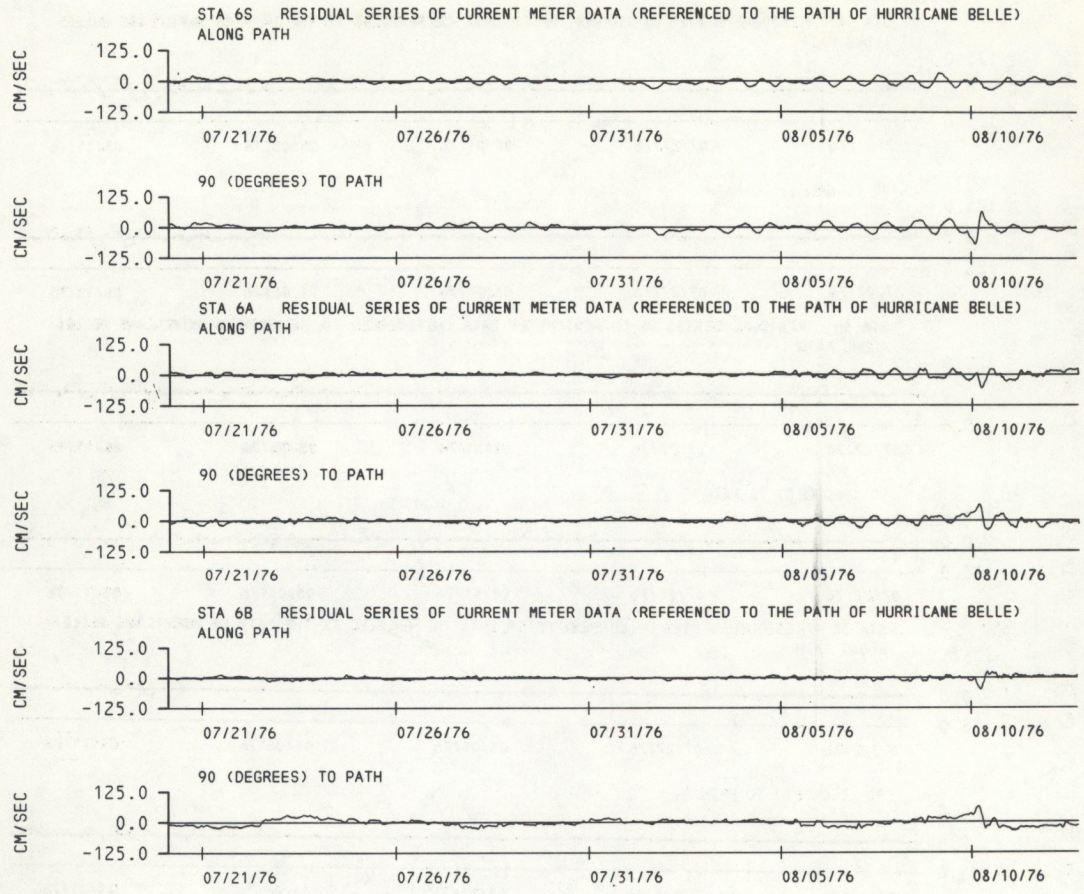

Figure 5. — Plots showing the residual currents resolved both along and at a 90-degree angle to the path of the hurricane—Continued.

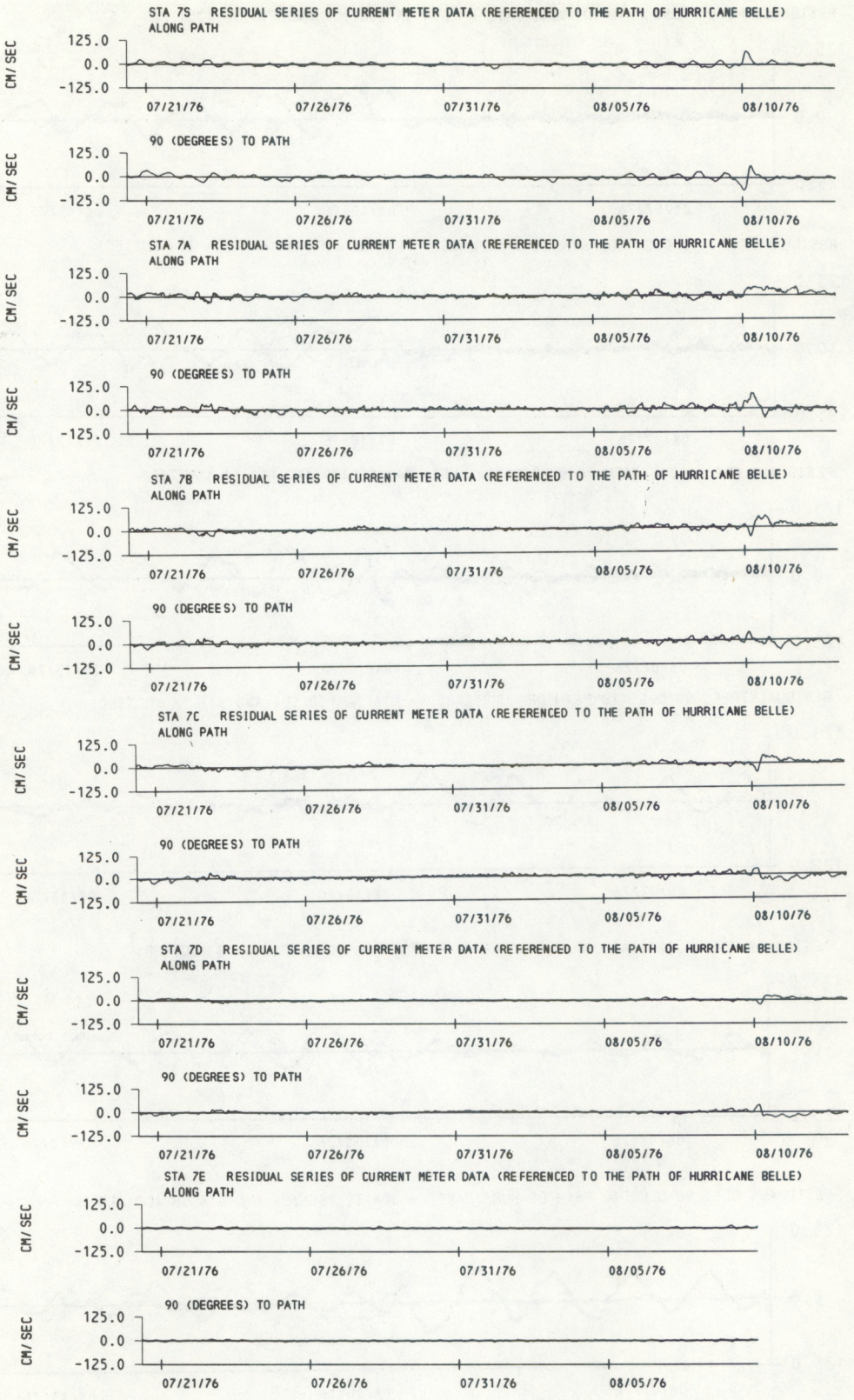

Figure 5. — Plots showing the residual currents resolved both along and at a 90-degree angle to the path of the hurricane.

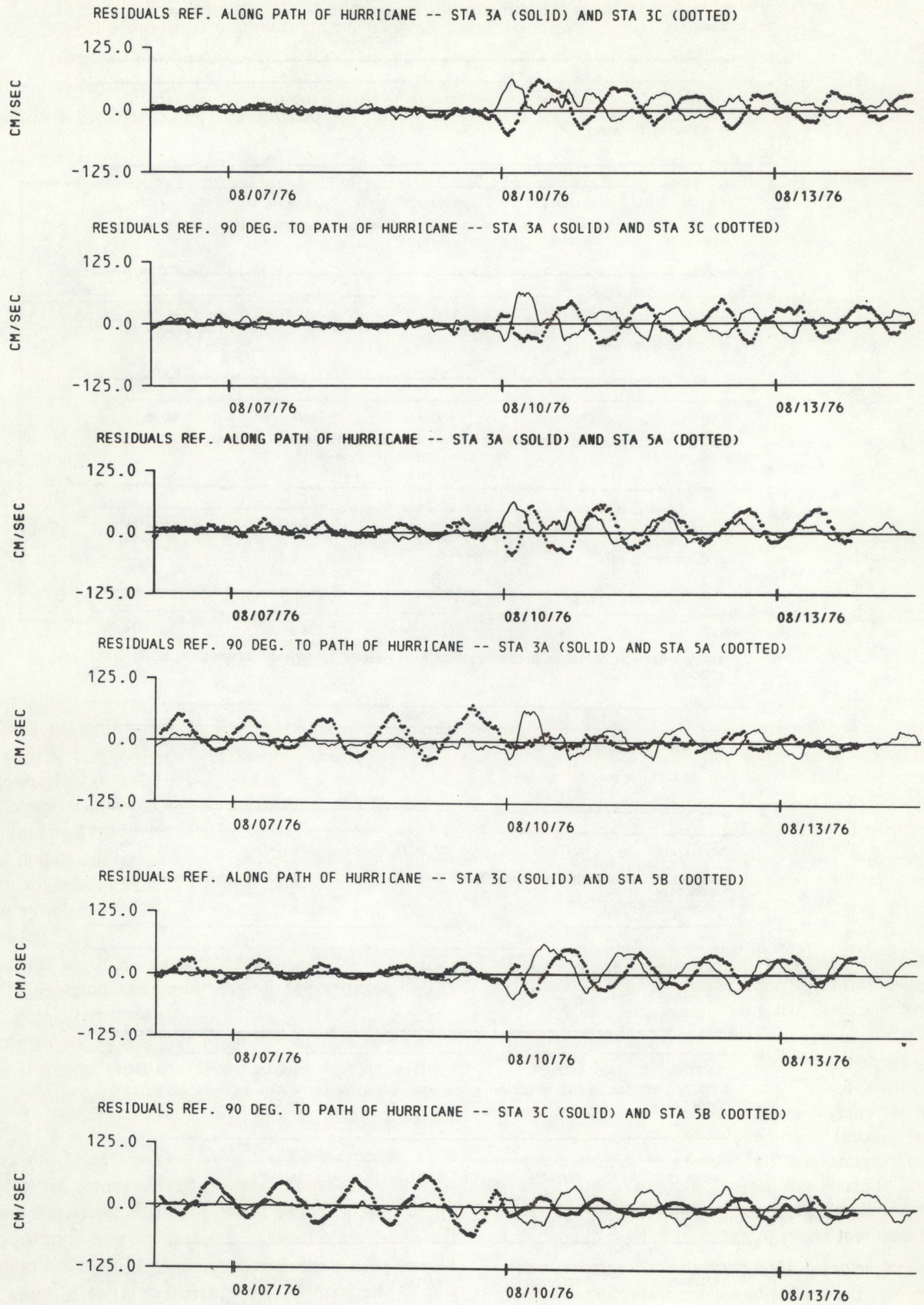

Figure 6. —Expanded time plots illustrating the baroclinic response at LT3 and LT5.

Table 3.—A classification of station locations according to bathymetry, distance from the path of the hurricane and observational levels. Respective to bathymetry, category 1 is less than 55 m; and category 2 is greater than 55 m. Respective to distance from the path, category 1 is directly in the path; and category 2 is to the right of the path. For observational levels, category 1 is above or within the thermocline; and category 2 is below the thermocline.

Current Meter Stations	Bathymetry	Path of the Hurricane	Observational Levels					
			S	A	B	C	D	E
LT1	1	2	-	-	1	2	2	-
LT2	1	1	-	1	2	2	-	-
LT3	2	2	-	1	1	2	2	-
LT4	1	2	1	1	2	2	-	-
LT5	2	2	-	1	2	2	-	-
LT6	2*	1	1	2	2	2	-	-
LT7	2*	2	1	1	2	2	2	2

* Indicates that these stations are in Hudson Canyon

excitation of near-inertial waves; however, except for the semidiurnal frequency, energy is enriched in the entire spectrum. For all other stations above or within the thermocline, except for station LT7S, the components resolved along the path of the hurricane indicate almost no enrichment of the near-inertial frequencies. However, for those stations, the component resolved at a 90-degree angle to the path of the hurricane indicates an order-of-magnitude increase at near-inertial frequencies. This agrees with all previous theoretical investigations, both analytically and numerically, which state, assuming a two-layer density regime, that in the upper layer the energy propagates tangentially to the meteorological disturbance. It is interesting to note that for all observational levels above or within the thermocline, except for LT6, an order-of-magnitude enrichment of the energy level for at least one component in the near-inertial frequency range is seen. At station LT6, no response to the passage of the hurricane is indicated. This is consistent with the conclusions in the water column response section which stated that mixing does not seem to occur at LT6.

Horizontal velocity field analysis

To resolve the spatial baroclinic response of the horizontal velocity field as Hurricane Belle passed through the New York Bight, a series of vector time splices was constructed. Using the categories in table 3, figure 8a represents time splices of the horizontal velocity field for the *upper layer* (above and within the thermocline), and figure 8b represents the horizontal velocity field for the *lower layer* (below the thermocline). The vectors represent the velocity of the residual current at the instantaneous time shown. The station location is at the end of the arrow, and the length of all arrows are linearly scaled to the maximum velocity observed. The maximum value of 87 cm s^{-1} occurred at LT3 at 0300 GMT 10 August 1976. At times the scaled vectors are longer than the boundary of the chart (i.e., at Station LT5); for these times, arrows are plotted without heads. The location of the hurricane (if it occurred during that given time splice) is indicated by a dot, and the progress of the hurricane is indicated by a dashed line.

In the *upper layer* before the passage of the hurricane, a weak southwestward flow is shown for stations on the shelf. Three hours after the hurricane enters the New York Bight, maximum current speeds up to 87 cm s^{-1} are attained, mainly in a direction tangential to the path of the hurricane. After 6 hours, an anti-cyclonic pattern in the southern region and a cyclonic pattern in the northern region develops. This

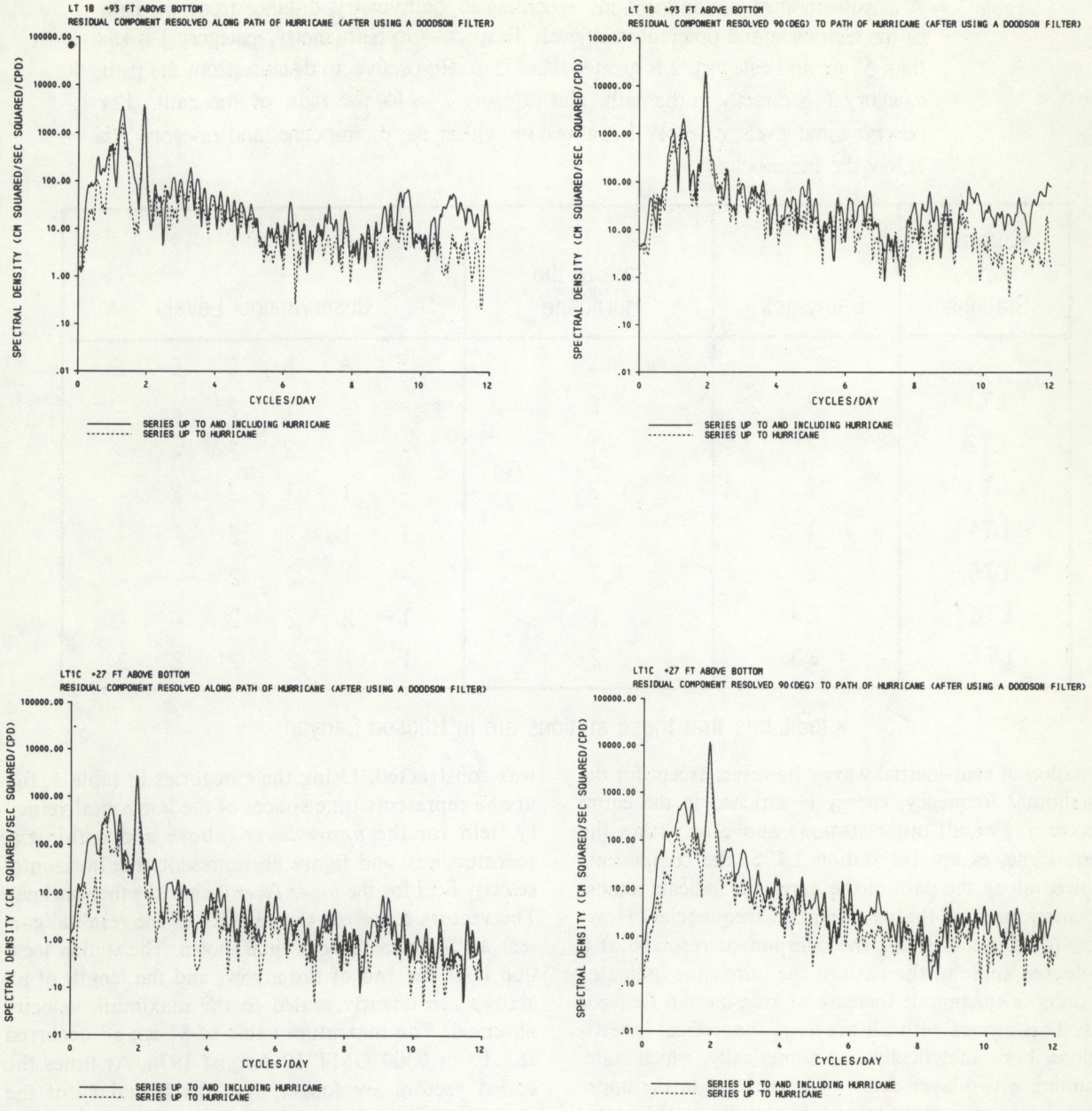

Figure 7. —After using a 39-hour Doodson filter, a calculated spectra for (1) the series up to and including the hurricane, and (2) the series up to the hurricane.

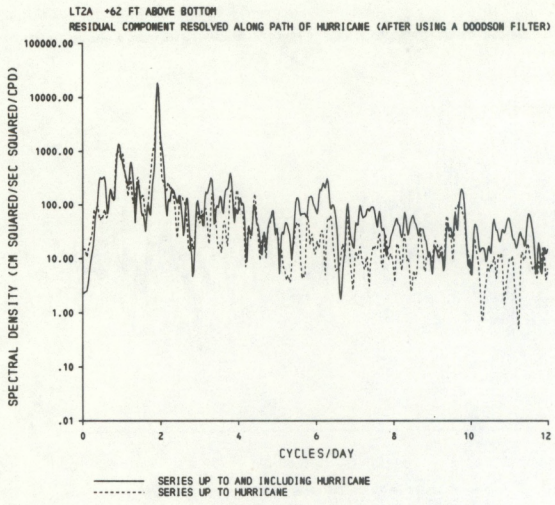

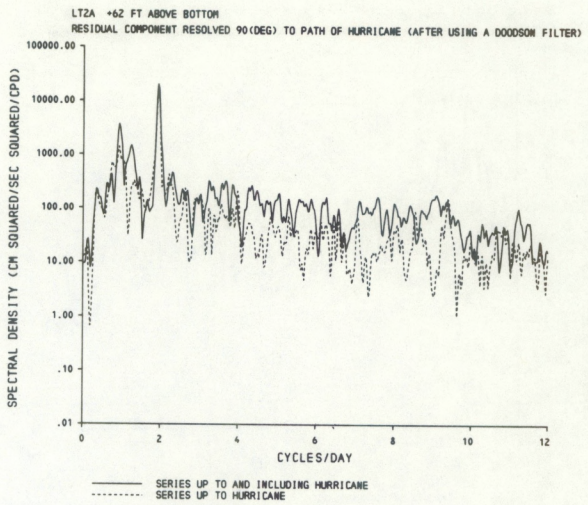

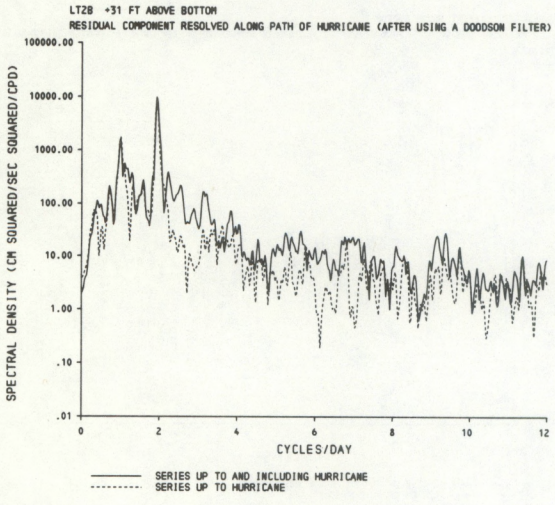

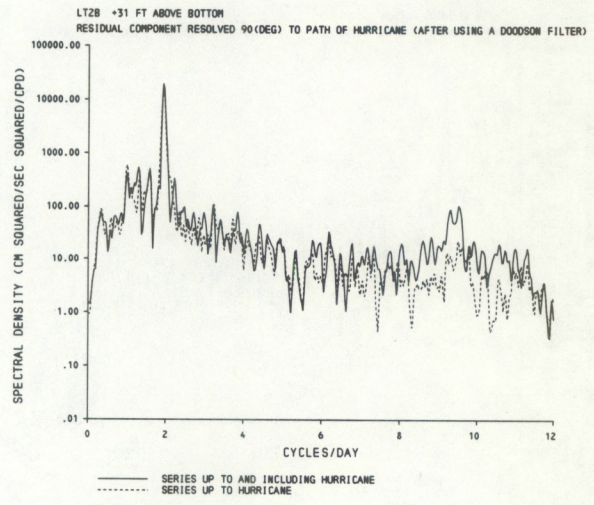

Figure 7. Calculated spectra after using a 39-hour Doodson filter—Continued.

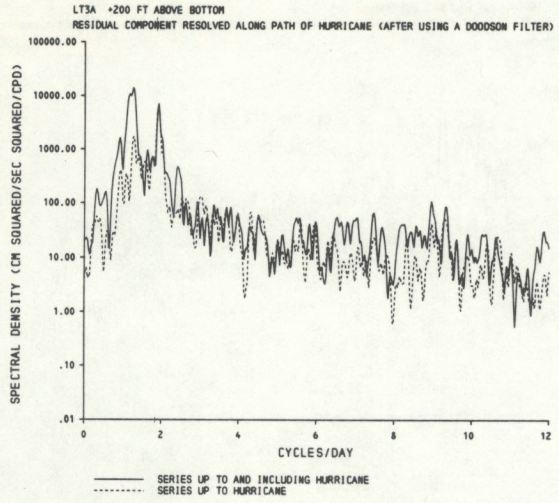

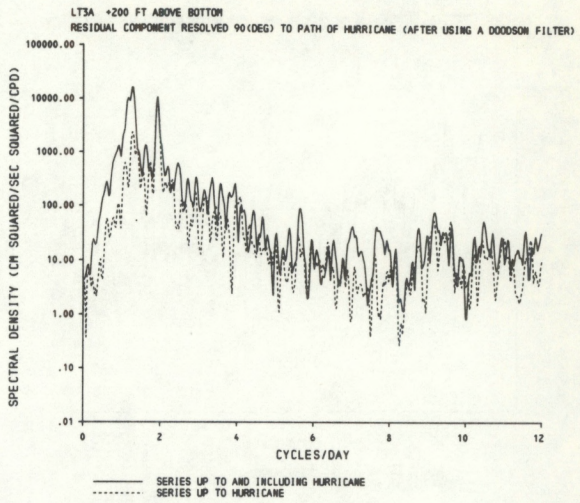

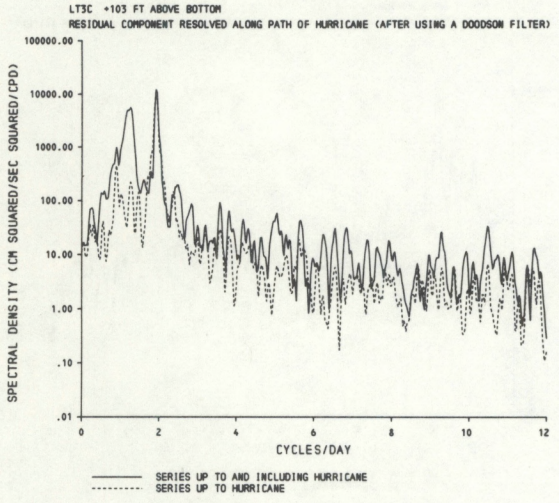

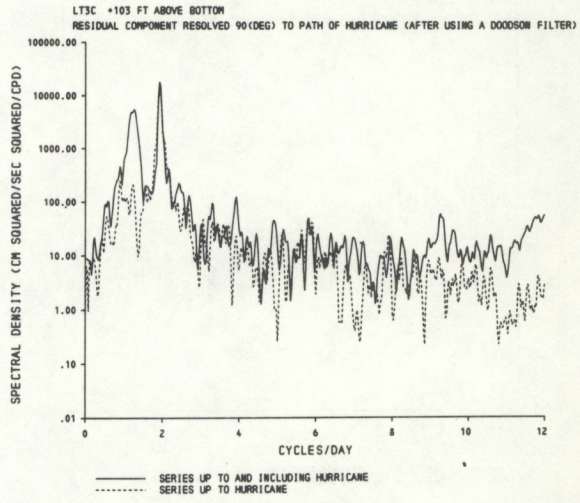

Figure 7. Calculated spectra after using a 39-hour Doodson filter—Continued.

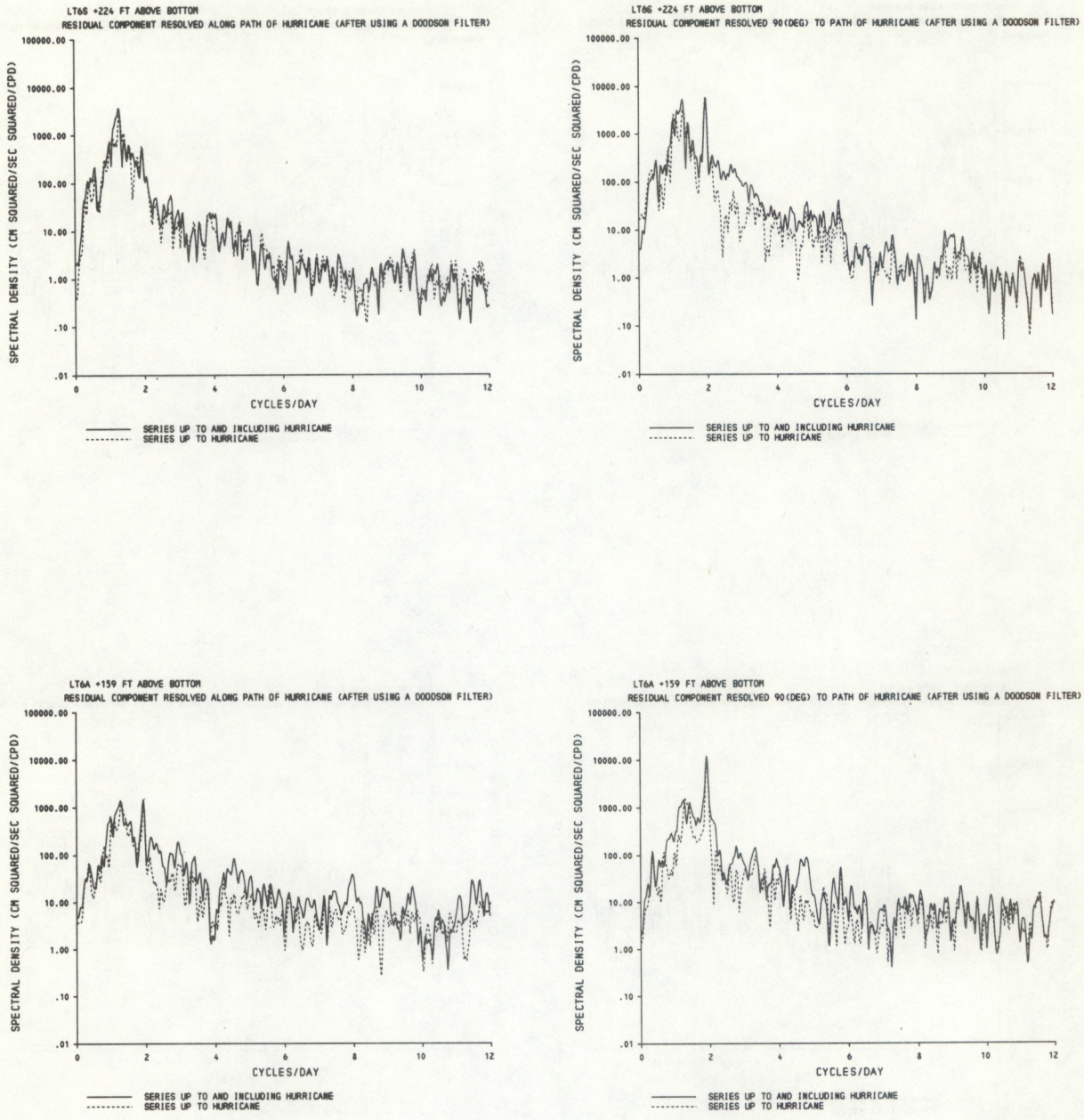

Figure 7. Calculated spectra after using a 39-hour Doodson filter—Continued.

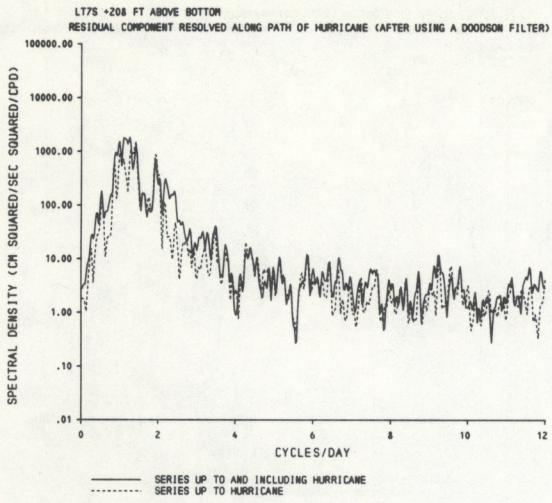

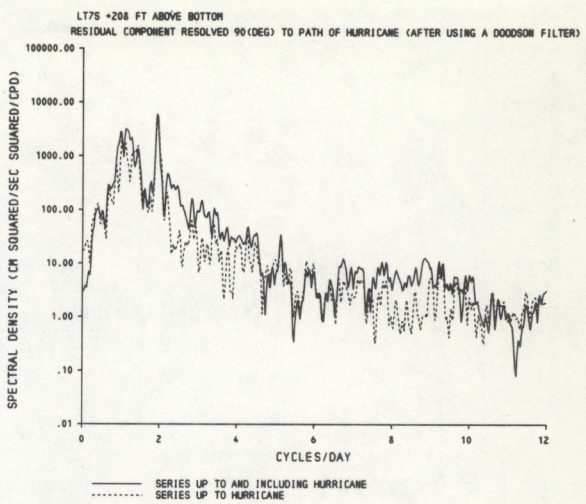

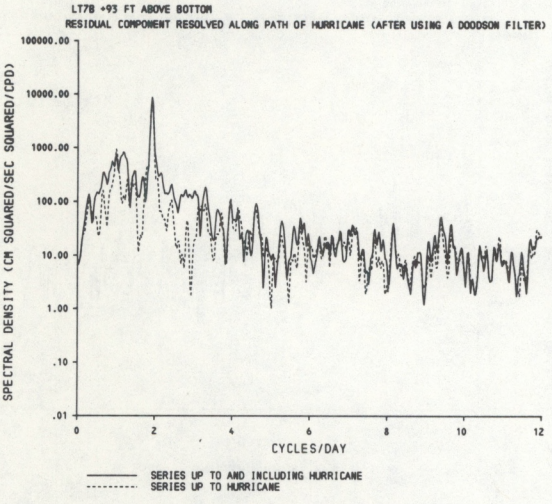

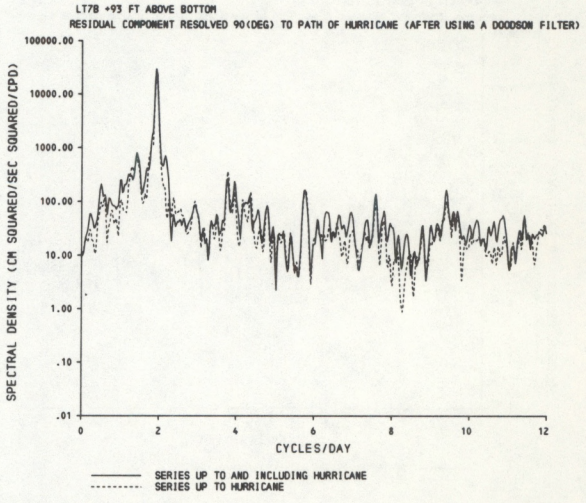

Figure 7. Calculated spectra after using a 39-hour Doodson filter—Continued.

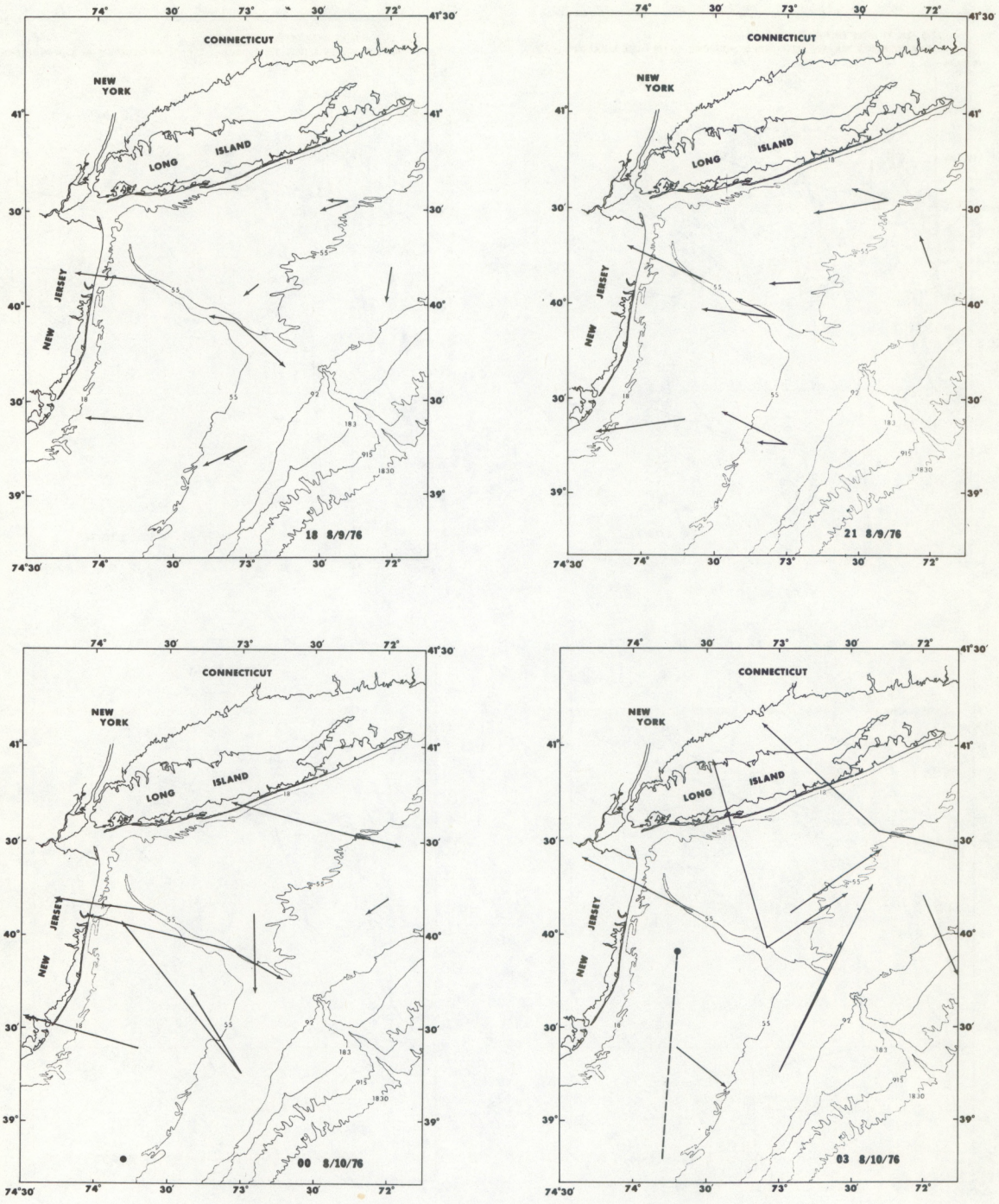

Figure 8a.—Time splices of the horizontal velocity field for the upper layer.

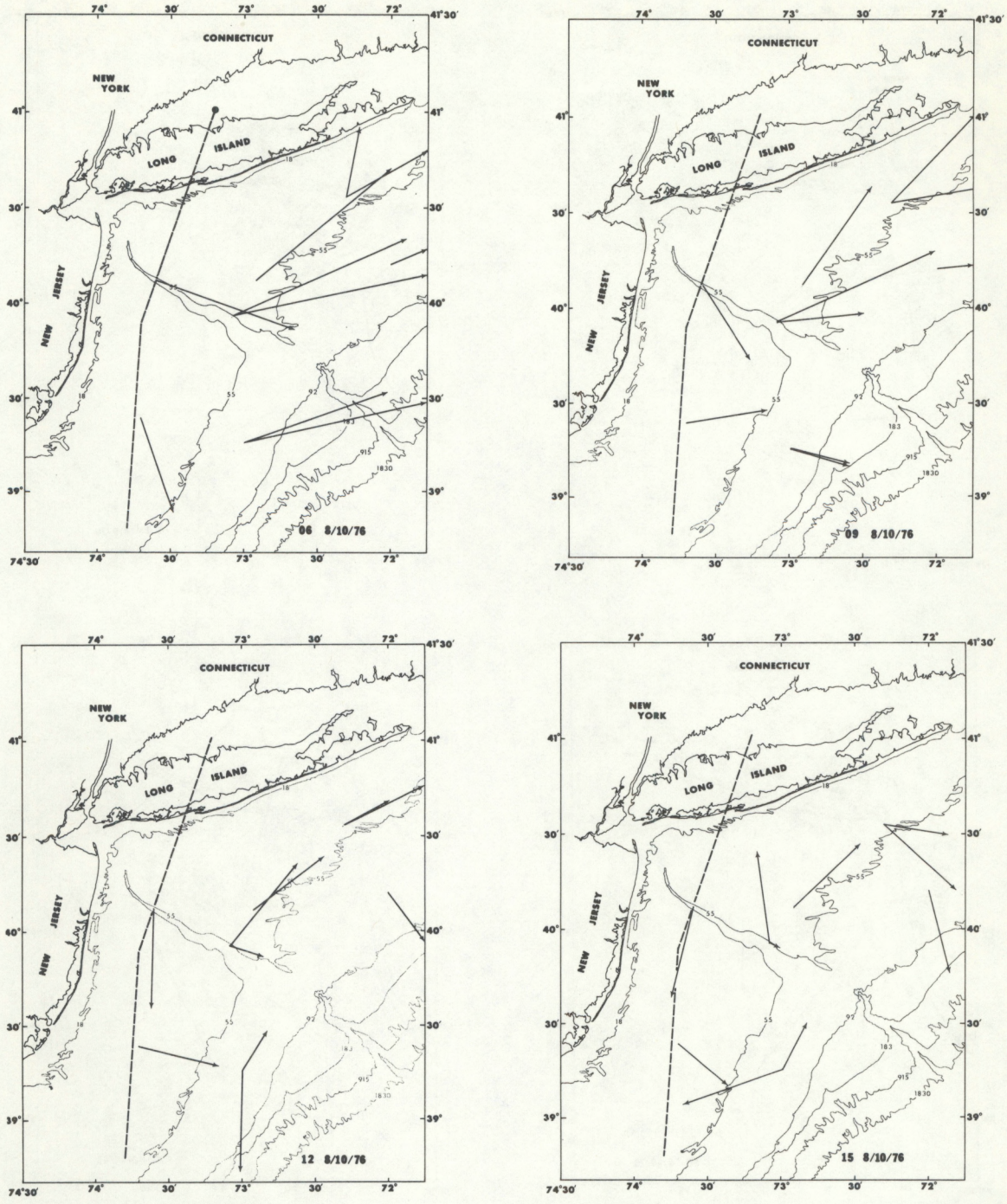

Figure 8a.—Time splices of the horizontal velocity field for the upper layer—Continued.

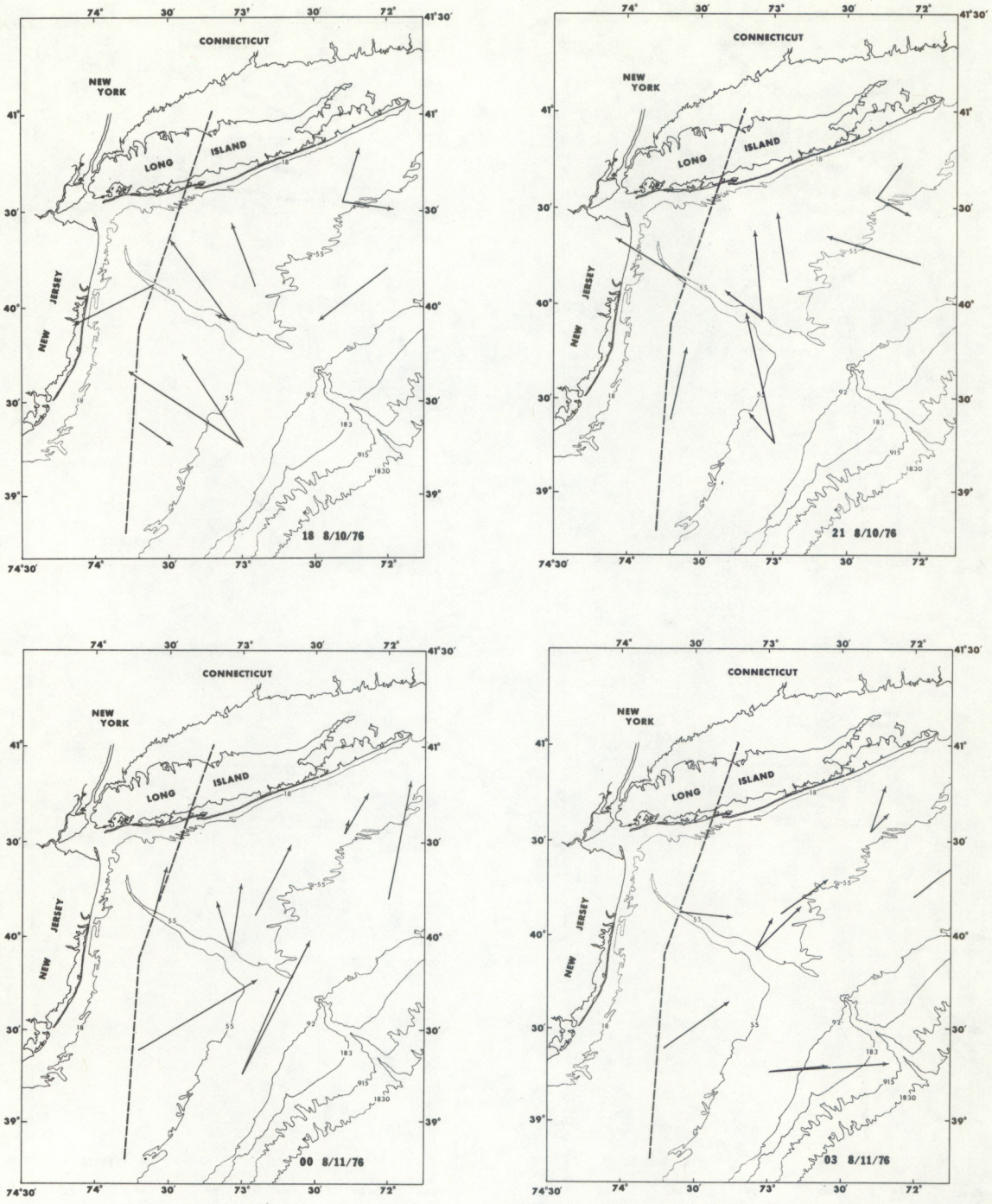

Figure 8a.—Time splices of the horizontal velocity field for the upper layer—Continued.

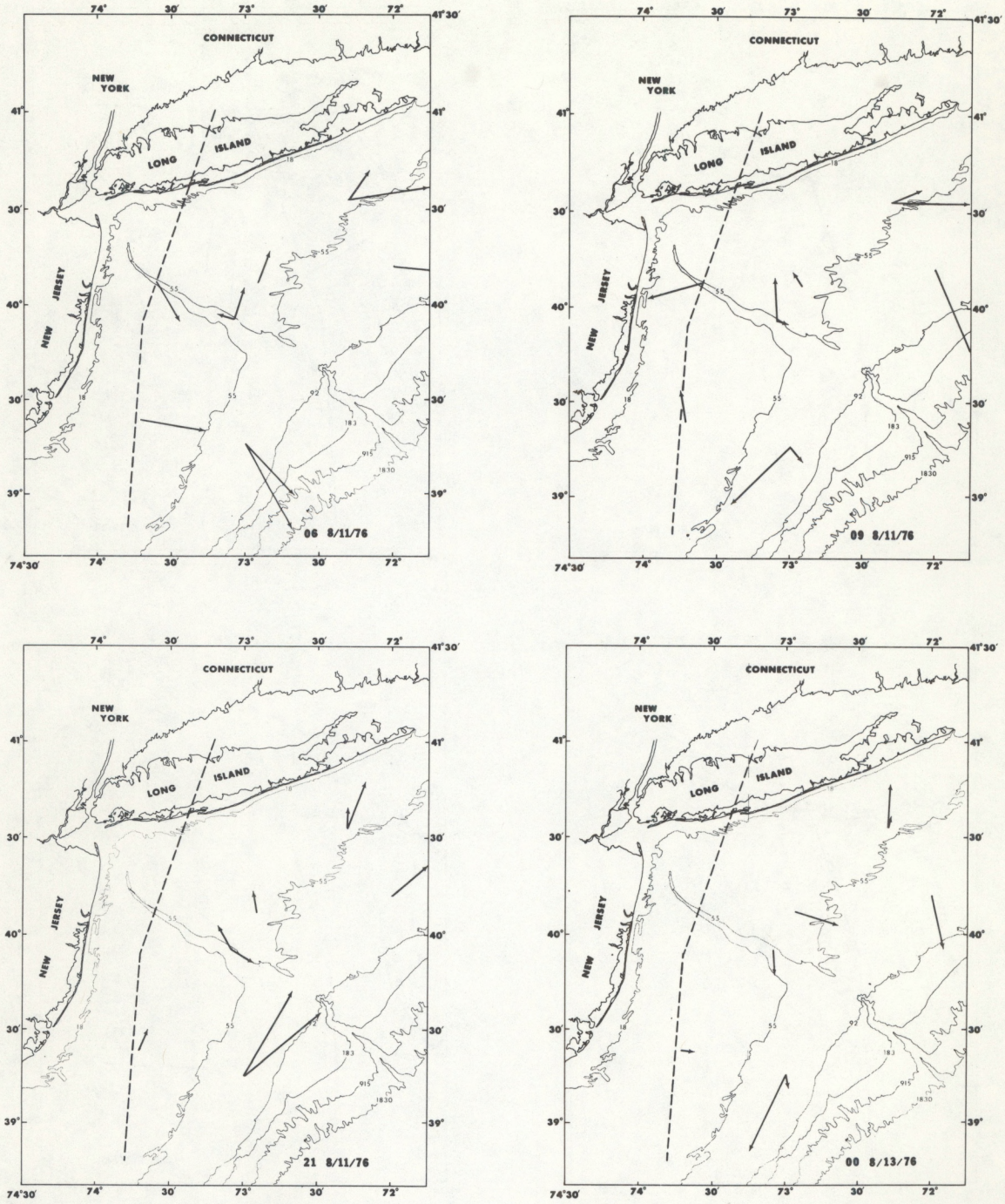

Figure 8a.—Time splices of the horizontal velocity field for the upper layer—Continued.

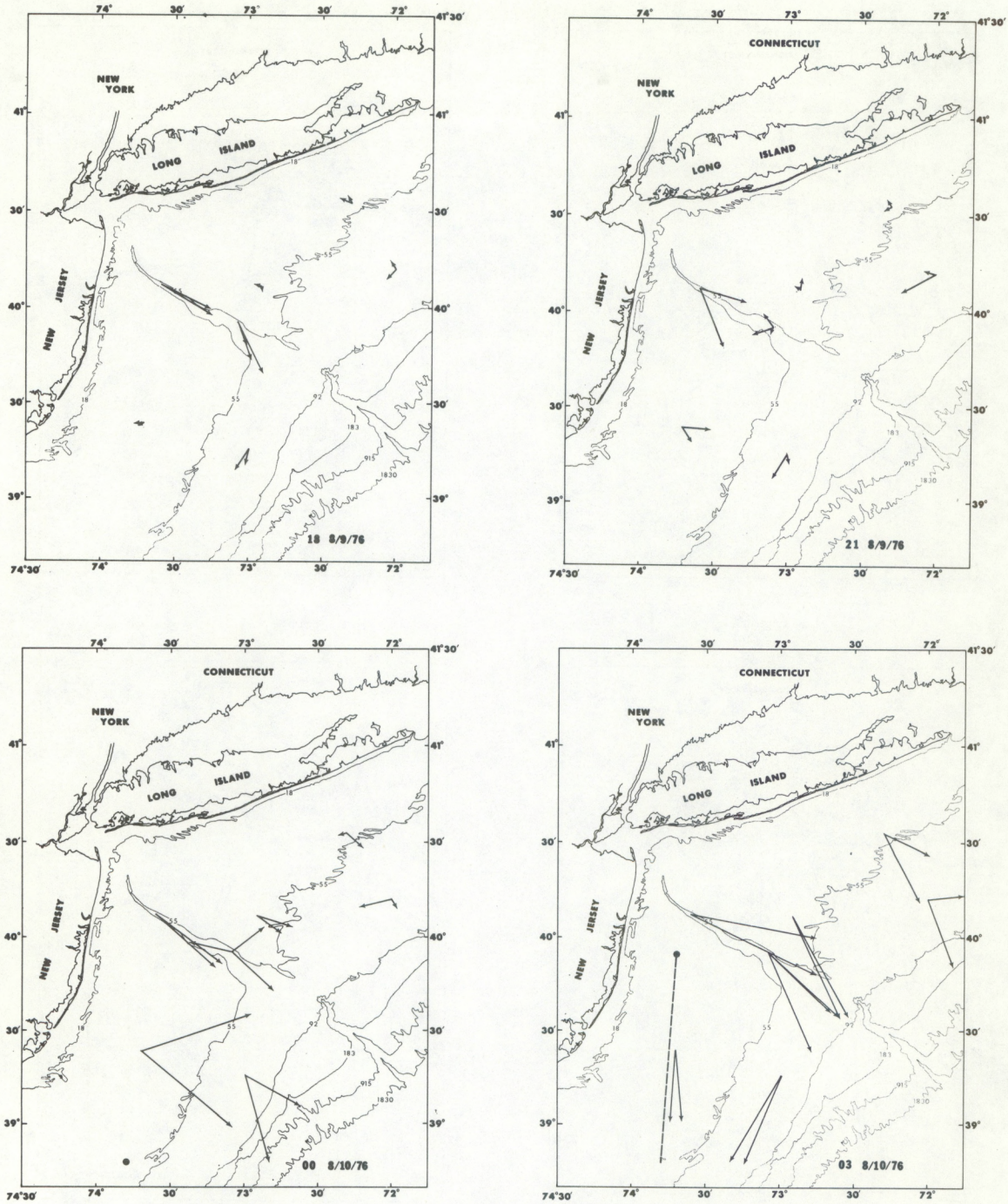

Figure 8b.—Time splices of the horizontal velocity field for the lower layer.

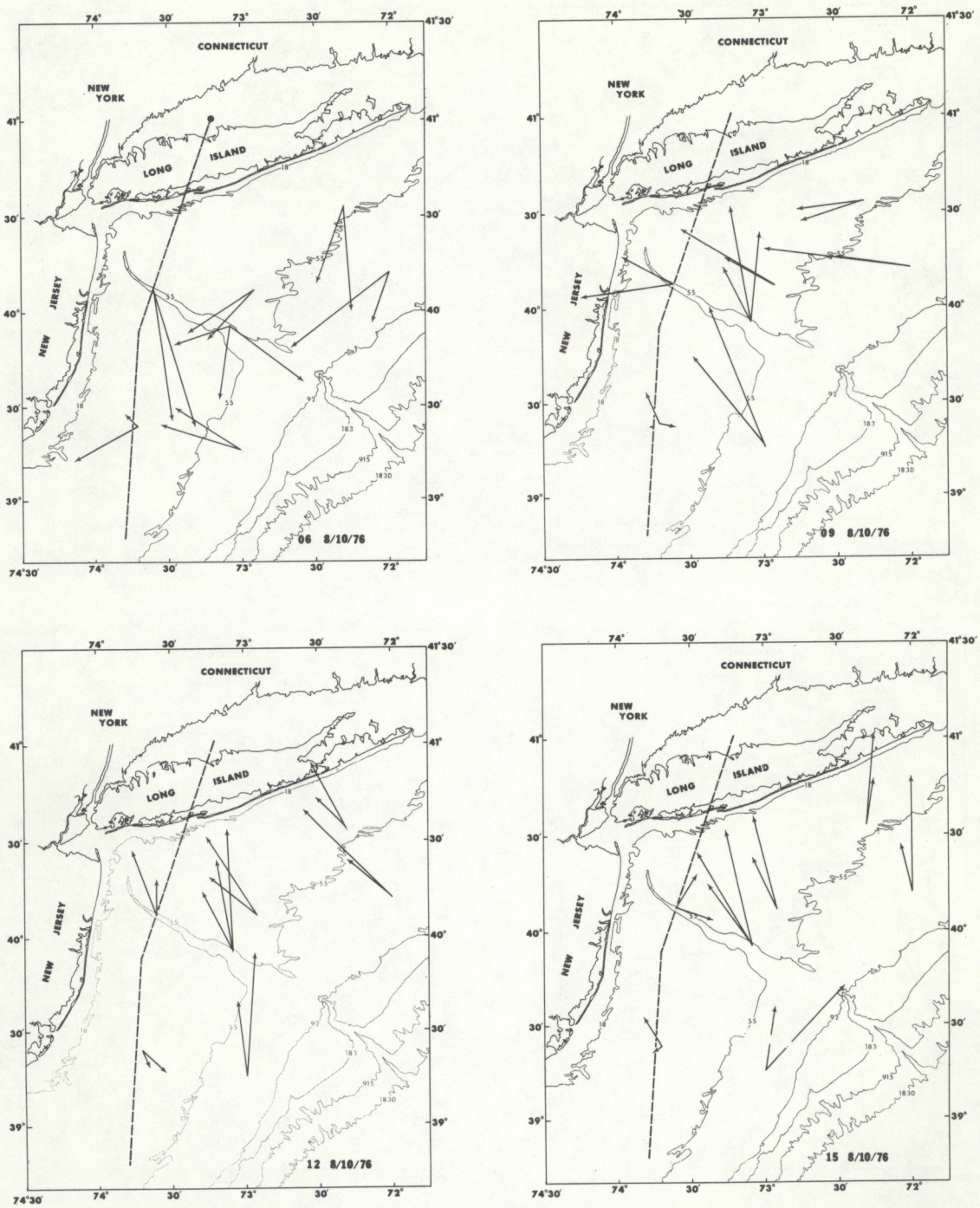

Figure 8b.—Time splices of the horizontal velocity field for the lower layer—Continued.

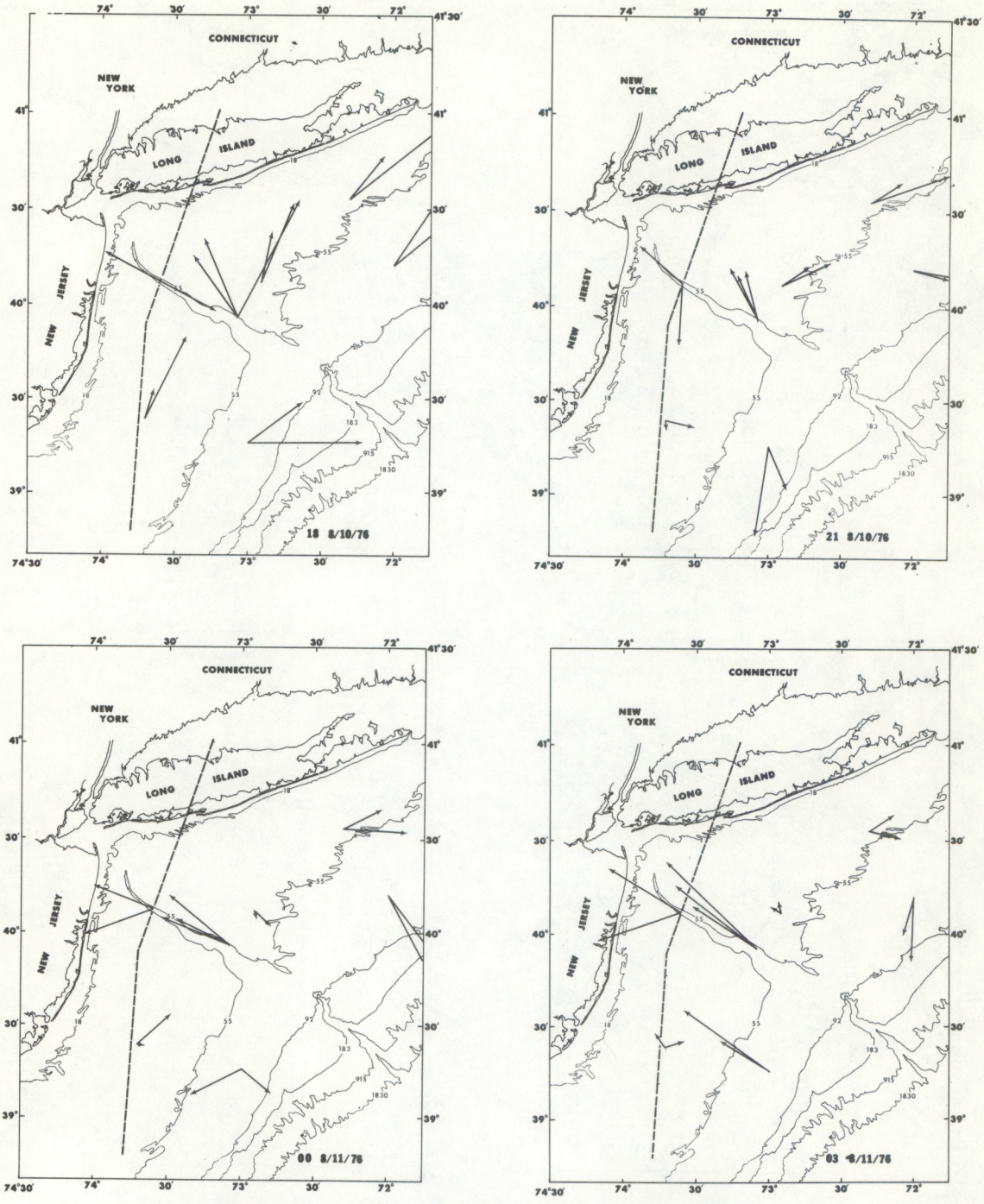

Figure 8b.—Time splices of the horizontal velocity field for the lower layer—Continued.

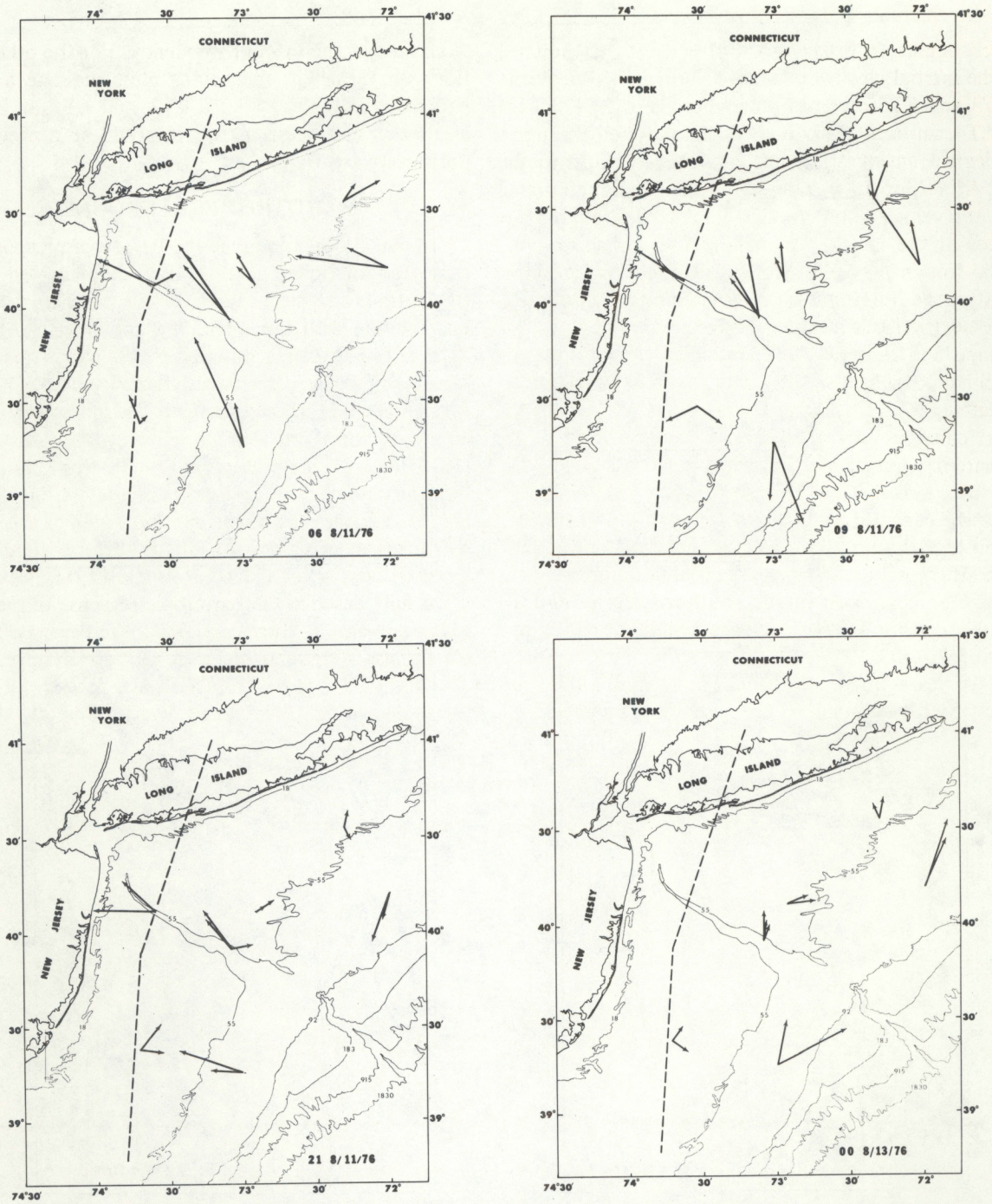

Figure 8b.—Time splices of the horizontal velocity field for the lower layer—Continued.

pattern begins to break down after 12 to 15 hours, and the inertial clockwise rotation through 360 degrees at LT3 and LT5 becomes pronounced. For LT1, LT2, and LT4, an oscillation at the inertial period through 180 degrees appears superimposed on a northeastward flow. At station LT6, after the passage of the hurricane, the velocity field rotates clockwise through 360 degrees at the inertial frequency. This behavior can also be seen in the spectra for LT6S where both before and after the hurricane passes the energy is confined to the near-inertial frequency band.

Chang and Anthes (1978) modeled the nonlinear, baroclinic response of the upper layer to hurricanes translating at 2.5, 5.0, and 10.0 m s^{-1}. For Cg = 1.0 m s^{-1}, a hurricane moving at 10.0 m s^{-1} is classified as a fast-moving hurricane. Hurricane Belle has previously been classified as a fast-moving hurricane. Their results are consistent with the observations. The results of their model after 20 hours is a response to the right of the storm with a strong tangential component. An anti-cyclonic pattern in the southern region and a cyclonic pattern in the northern region develops in the model area.

In the *lower layer* at stations LT3 and LT5, the velocity fields respond to the hurricane by rotating clockwise at the inertial frequency. For the other stations on the shelf, the vector plots indicate a weak baroclinic response. At LT1, LT2, and LT4, an inertial oscillation can be seen superimposed on a prevailing northeastward flow.

BAROTROPIC RESPONSE

Geisler (1970) describes the barotropic response to a moving hurricane as an "initial deformation in the free surface height produced by the pressure anomaly and moving with the storm," which is followed by a "barotropic divergence forced by the wind stress curl. This leads to a geostrophically balanced trough in the free surface height" and finally a "dissolution by planetary wave radiation takes place." According to Geisler (1970) and Longuet-Higgins (1965), this dissolution into the planetary waves occurs in about 1 day. Kŕaus (1972) describes the barotropic response of the ocean to storms as a breakdown of the surface trough into localized quasi-geostrophic barotropic Rossby waves.

To fully describe the barotropic response of the shelf to the passage of Hurricane Belle, the response of the sea surface is required. Figure 9 represents the response of the OTTS I gage (from Gill and Porter, 1978) to the passage of Hurricane Belle. The results at

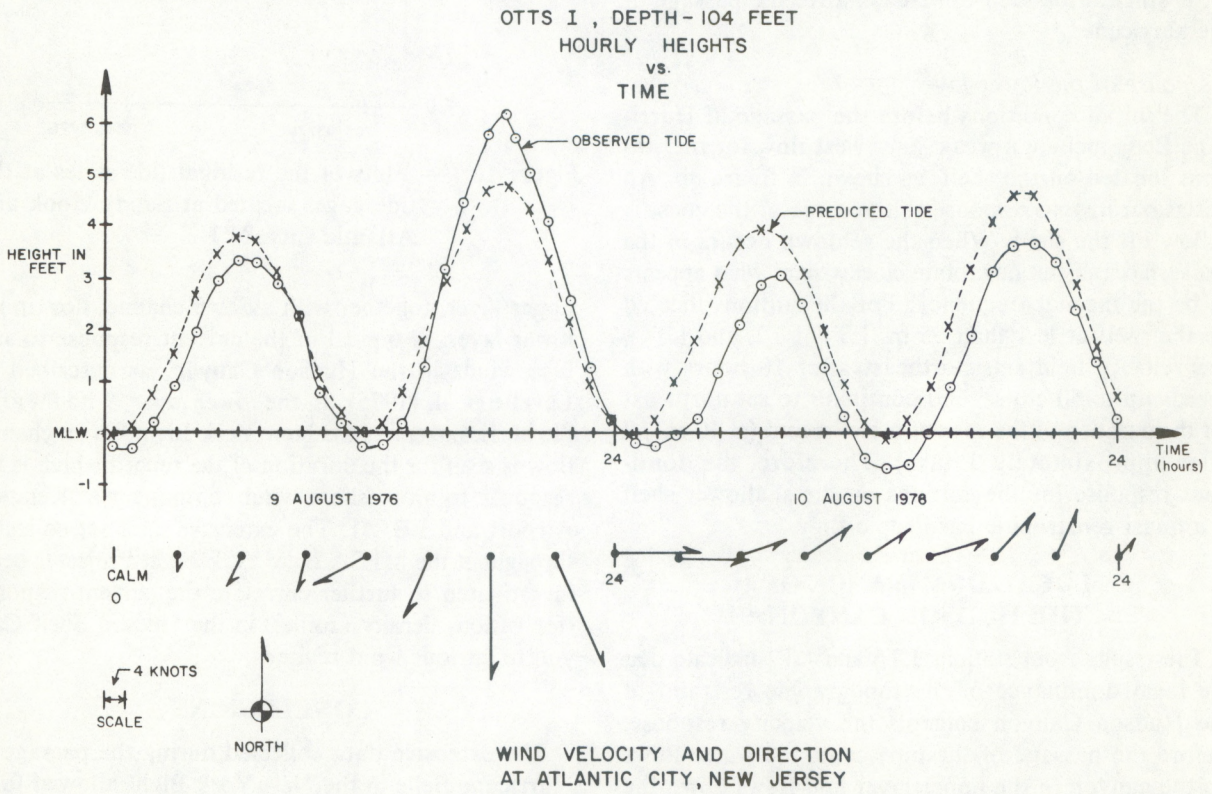

Figure 9. — Plot of the observed and predicted series at the OTTS 1 gage. Wind data at Atlantic City, N.J., are also illustrated.

OTTS II are almost identical. However, at the DELMARVANC DSTG, the sea surface measurements do not indicate a response to the passage of the hurricane. Figure 10 illustrates the response to the hurricane at the tide gages located at Sandy Hook and Atlantic City, N.J. The residuals are calculated in the same manner as the current meter residuals. Both figures illustrate the classical initial surge at the coast, then a trough developing relative to the level before the passage of the hurricane.

Response to the upper layer

Analytical and numerical investigations to describe the response of the ocean to the passage of a storm usually consider a two-layer ocean where the upper layer is well mixed and a flat bottom layer is assumed to be deep and motionless. These assumptions filter the barotropic response. A wind profile is imposed on the surface, and a storm translation speed is specified. Observations shown in figure 8a indicate the importance of the barotropic response for the station on the shallow shelf. Initially, the baroclinic response is dominant; then after 20 hours, the barotropic response dominates the horizontal velocity field. Both the residual time plots and the time splices indicate a northeastward flow. Thirty-two hours after the passage of the storm, this northeastward flow becomes weaker; however, it still can be seen for 2 days after the passage of the hurricane.

Response of the lower layer

The initial conditions before the passage of Hurricane Belle include a weak southwest flow for the stations located on the shelf, as shown in figure 8b. An initial barotropic response to the surge at the coast is a flow off the shelf. When the setdown occurs in the sea surface, all stations rotate clockwise at what appears to be the inertial frequency. For the stations located on the shelf at less than 55 m (LT1, LT2, and LT4), the velocity field sets northeast after 18 hours with speeds up to 50 cm s^{-1} and continues to set northeast for the duration of the current meter record (at 10 cm s^{-1} after approximately 3 days). Therefore, the dominant response for the stations on the shallower shelf is a quasi-geostrophic barotropic flow.

LOCAL DOMINANCE OF THE HUDSON CANYON

The results from stations LT6 and LT7 indicate that the local dominance of the topographic restraint of the Hudson Canyon controls the velocity response. Before the passage of the hurricane, the water flows up the canyon in the upper layer and flows down the canyon in the lower layer. The up-channel flow in the

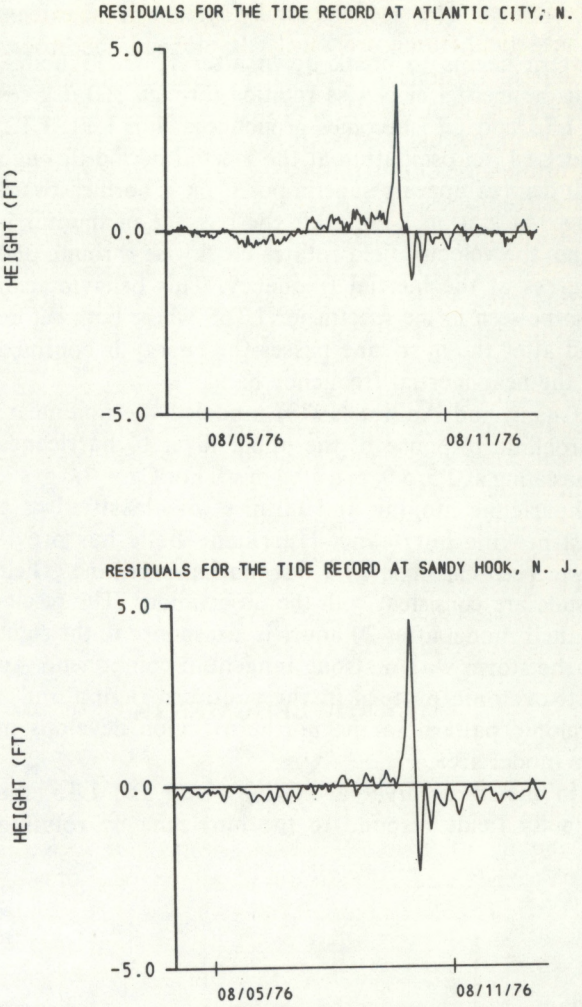

Figure 10. — Plots of the residual tide series at the tide gages located at Sandy Hook and Atlantic City, N.J.

upper layer, together with a down-channel flow in the lower layer, is typical of the current response to surface winds in the Hudson Canyon, as described by Lavelle et al. (1975). In the *lower layer,* 9 hours after the hurricane enters the New York Bight, an up-channel flow is seen for the duration of the record which is the response to an offshore wind component at Kennedy Airport and EB- 41. The extensive data set collected throughout the MESA New York Bight Project is being investigated to further correlate the current response (for various density profiles) in the Hudson Shelf Canyon to various wind regimes.

CONCLUSIONS

The extensive data collected during the passage of Hurricane Belle in the New York Bight allowed for a complete description of the response of the shelf to be

performed. The results generally agree with the extensive theoretical frame previously developed. The observations at stations LT3 and LT5 indicate a baroclinic response for a two-layered density regime (the generation of internal inertia-gravity waves) to a fast-moving storm as the dominant feature. For these stations, the barotropic response was of a secondary significance. However, for the other station locations, the results indicate the importance of the barotropic response. At stations LT1, LT2, and LT4, the baroclinic response is masked by the barotropic response and can be seen mainly in the velocity component resolved at a 90-degree angle to the path of the hurricane. The result can be quite important in further hurricane model development. The initial condition usually specified by modelers filters out the barotropic response. These data verify the results of the existing models in describing the baroclinic response; however, these data also indicate the significance of the barotropic response. At stations LT6 and LT7, the local effect of the Hudson Canyon is seen, especially in the lower layer.

ACKNOWLEDGMENTS

We are grateful to Brenda Via for assisting in the processing of the current meter data collected as part of the MESA New York Bight Project; to Michael Connolly and Gary Dingle for helping in the preparation of the extensive illustrations presented in this report; and to John Roseborough for photographic assistance. We also thank Charles R. Muirhead for his administrative support throughout the project. We thank the many individuals in the National Ocean Survey and the National Weather Service who contributed the tide and meteorological information. We especially thank Sondra Burman for typing the tables and text of this report. This work was supported by the National Ocean Survey and the Marine Ecosystem Analysis Program of the National Oceanic and Atmospheric Administration.

REFERENCES

Black, P. G., and W. D. Mallinger, 1972: The mutual interaction of Hurricane Ginger and the upper mixed layer of the Ocean, 1971. *Project Stormfury Annual Report,* U.S. Department of Commerce, Washington, D.C., 63-87.

Chang, S. W., and R. A. Anthes, 1978: Numerical simulations of the ocean's nonlinear, baroclinic response to translating hurricanes. *J. Phys. Oceanogr.,* 8, 468-480.

Cooley, J. W., and J. W. Tukey, 1965: An algorithm for the machine calculation of complex Fourier series. *Mathe. of Comp.,* 19, No. 19.

Elsberry, R., T. Fraim, and R. Trapnell, Jr., 1976: A mixed layer model of the oceanic thermal response to hurricanes. *J. Geophy. Res.,* 81, 1153-1162.

Geisler, J. E., 1970: Linear theory of the response of a two layer ocean in a moving hurricane. *Geophys. Fluid Dyn.,* 1, 249-272.

Geisler, J. E., and R. F. Dickinson, 1972: The role of variable coriolis parameter in the propagation of inertia-gravity waves during the process of geostrophic adjustment. *J. Phys. Oceanogr.,* 2, 263-272.

Gill, S., and D. L. Porter, 1978: Theoretical offshore tide range derived from a simple Defant tidal model compared with observed offshore tides. *International Hydrographic Review* (in press).

Gray, W. M., 1966: On the scales of motion and internal stress characteristics. *J. Atmos. Sci.,* 23, 278-288.

Hazelworth, J. B., 1968: Water temperature variations resulting from hurricanes. *J. Geophy. Res.,* 73, 5105-5123.

Hazelworth, J. B., S. R. Cummings, S. M. Minton, and G. A. Berberian, 1977: MESA New York Bight Project, Expanded Water Column Characterization Cruise (XWCC11) of the NOAA Ship RESEARCHER, September, 1976: *NOAA Data Report ERL MESA,* 29.

Ichiye, T., 1977: Response of a two-layer ocean with a baroclinic current to a moving storm, Part I. Quasi-geostrophic baroclinic motion. *J. Oceanogr. Soc.,* Japan, 33, 151-160.

Kŕaus, E. B., 1972: *Atmosphere-ocean Interaction.* Clarendon Press, Oxford.

Landis, R. C., and D. F. Leipper, 1968: Effects of Hurricane Betsy upon Atlantic Ocean temperature, based upon radio-transmitted data. *J. Appl. Meteor.,* 7, 554-562.

Lavelle, J. W., G. H. Kéller, and T. L. Clarke, 1975: Possible bottom current response to surface winds in the Hudson shelf channel. *J. Geophys. Res.,* 80, 1953-1955.

Lawrence, M. B., 1976: North Atlantic tropical cyclones, 1976. *Mariners Weather Log.*

Leipper, D. F., 1967: Observed ocean conditions and Hurricane Hilda 1964. *J. Atmos. Sci.,* 24, 182-196.

Longuet-Higgins, M. S., 1965: The response of a stratified ocean to stationary or moving wind systems. *Deep Sea Res.,* 12, 923-973.

McFadden, J. D., 1967: Sea-surface temperatures in the wake of Hurricane Betsy (1965). *Monthly Weather Review,* 95, 299-302.

Mooers, C. N. K., 1976: Physical variability of the continental shelf, *Mem. Soc. Roy. Sci.,* Leige, 10, 27-30.

National Oceanic and Atmospheric Administration, 1975: Hurricane Eloise: The Gulf Coast. *Natural Disaster Survey Report* 75-1.

NOAA, 1976: Hurricane Belle, Climatological Data. *National Summary,* 27, 4-7.

NOAA, 1976: *Local Climatological Data* (Monthly Summary), National Weather Service OFC, JFK Intl. Airport, June-October.

O'Brien, J. J., 1967: The nonlinear response to a two-layer baroclinic ocean to a stationary, axially-symmetric hurricane, Part II. Upwelling and mixing induced by momentum transfer. *J. Atmos. Sci.,* 24, 280-315.

O'Brien, J. J., 1968: The response of the ocean to a slowly moving cyclone. Paper presented at the VOMG-DGG-AMS-RMS Joint Meeting, Hamburg, April 1968.

O'Brien, J. J., and R. V. Reid, 1967: The nonlinear response to a two-layer baroclinic ocean to a stationary, axially-symmetric hurricane: Part I. Upwelling induced by momentum transfer. *J. Atmos. Sci.,* 30, 558-567.

Perlroth, I., 1965: Hurricane behavior as related to oceanographic environmental conditions. *Tellus,* 19, 258-267.

Roberts, J., 1975: *Internal Gravity Waves in the Ocean,* New York, Dekker.

Schott, F., 1971: Spatial structure of inertial-period motions in a two-layered sea, based on observations. *J. Mar. Res.* 29, 85-101.

Shuleykin, V. V., 1970: The power of a tropical hurricane as a function of the underlying sea surface temperature. *Atmos. and Oceanic Phys.,* 6, 1219-1237.

Smith, P. C., B. Petrie, and C. R. Mann, 1978: Circulation, variability, and dynamics of the Scotian shelf and slope. *Fish. Res. Board, Canada,* 35, 1067-1083.

Starr, R. B., J. B. Hazelworth, S. R. Cummings, and G. A. Berberian, 1977: MESA New York Bight Project, Expanded Water Column Characterization Cruise (XWCC 10) of the NOAA Ship GEORGE B. KELEZ, 28 June-1 July, 1976. *NOAA Data Report ERL,* MESA, 28.

(Continued from inside front cover)

NOS 67 NGS-3. Algorithms for computing the geopotential using a simple-layer density model. Foster Morrison, March 1977, 41 pp. (PB266967)

NOS 68 NGS-4. Test results of first-order class III leveling. Charles T. Whalen and Emery Balazs, November 1976, 30 pp. (PB265421)

NOS 69 Tidal hydrodynamics in the Strait Juan de Fuca - Strait of Georgia. Bruce B. Parker, January 1977, 56 pp. (PB270191)

NOS 70 NGS-5. Selenocentric geodetic reference system. Frederick J. Doyle, A. A. Elassal, and J. R. Lucas, February 1977, 53 pp. (PB266046)

NOS 71 NGS-6. Application of digital filtering to satellite geodesy. C. C. Goad, May 1977, 73 pp. (PB270192)

NOS 72 NGS-7. Systems for the determination of polar motion. Soren W. Henriksen, May 1977, 55 pp. (PB274698/AS)

NOS 73 NGS-8. Control leveling. Charles T. Whalen, May 1978, 23 pp. (PB286838)

NOS 74 NGS-9. Survey of the McDonald Observatory radial line scheme by relative lateration techniques. William E. Carter and T. Vincenty, June 1978, 33 pp. (PB287427)

NOS 75 NGS-10. An algorithm to compute the eigenvectors of a symmetric matrix. E. Schmid, August 1978, 5 pp. (PB287923)

NOS 76 NGS-11. The application of multiquadric equations and point mass anomaly models to crustal movement studies. Rolland L. Hardy, November 1978, 63 pp. (PB293544)

NOS 77 Numerical simulation of sedimentation and circulation in rectangular marina basins. David R. Askren, January 1979, 137 pp. (PB294107)

NOS 78 Wave sensors survey. Richard L. Ribe, July 1979, 48 pp. (PB80 118581)

NOS 79 NGS-12. Optimization of horizontal control networks by nonlinear programing. Dennis Milbert, August 1979 42 pp. (PB80 117948)

NOS 80 Circulation and hydrodynamics of the Lower Cape Fear River, North Carolina. Joseph M. Welch and Bruce B. Parker, August 1979, 117 pp. (PB80 117088)

NOS 81 Formulas for positioning at sea by circular, hyperbolic, and astronomic methods. James Collins, February 1980, 30 pp.

NOS 82 NGS-13. Feasibility Study of the Conjugate Gradient Method for Solving Large Sparse Equation Sets. Lothar Grundig

NOS 83 NGS-14. Tidal Corrections to Geodetic Quantities. Peter Vanicek

NOS 84 NGS-15. Application of Special Variance Estimators to Geodesy. John D. Bossler, February 1980

NOS 85 NGS-16. The Bruns Transformation and a Dual Setup of Geodetic Observational Equations. Erik W. Grafarend, April 1980

NOS 86 NGS-17. On the Weight Estimation in Leveling. Peter Vanicek and Erik W. Grafarend, May 1980

NOS 87 NGS-18. Crustal Movement Investigation at Tejon Ranch, Calif. Richard A. Snay and Michael W. Cline, June 1980

NOS 88 NGS-19. Horizontal Control Surveys. Joseph F. Dracup, June 1980